# The novel (1,3)β-D-glucan synthase catalytic subunit Bgs4p from fission yeast is essential during both cytokinesis and polarized growth.

**Juan Carlos G. Cortés[1], Elena Carnero[1], Junpei Ishiguro[2], Yolanda Sánchez[1], Angel Durán[1] and Juan Carlos Ribas[1]***

[1]Instituto de Microbiología Bioquímica and Departamento de Microbiología y Genética, Consejo Superior de Investigaciones Científicas (CSIC) / Universidad de Salamanca, 37007 Salamanca, Spain.

[2]Department of Biology, Faculty of Science and Engineering, Konan University, Okamoto 8-9-1, Kobe 658-8501, Japan.

**Running title:** Bgs4 is essential for cytokinesis and cell growth

**Key words:** Cell integrity / Cell wall / Cytokinesis / Fission Yeast / Glucan / (1,3)-β-D-Glucan Synthase

* Corresponding author address:

Instituto de Microbiología Bioquímica.

Edificio Departamental, room # 222.

Campus Miguel de Unamuno.

CSIC / Universidad de Salamanca.

37007 Salamanca. Spain.

Phone: (34) 923-294733, Fax: (34) 923-224876, E-mail: ribas@usal.es

**ABSTRACT**

*Schizosaccharomyces pombe* contains four putative (1,3)β-D-glucan synthase (GS) catalytic subunits, Bgs1p to Bgs4p. In this work, we cloned *bgs4*$^+$ and show that Bgs4p is the only subunit 1) essential for maintaining cell integrity during both cytokinesis and polarized growth, and 2) found to be part of the GS enzyme. Here we show that *bgs4*$^+$, *cwg1*$^+$ (*cwg1-1* shows reduced cell-wall β-glucan and GS catalytic activity) and *orb11*$^+$ (*orb11-59* is defective in cell morphogenesis) are the same gene. *bgs4*$^+$ is essential during spore germination. *bgs4*$^+$ shut-off produces cell lysis at growing poles and mainly at the septum prior to cytokinesis, suggesting that Bgs4p is essential for cell wall growth and for compensating an excess of cell wall degradation during cytokinesis. Shut-off and overexpression analysis suggest that 1) Bgs4p forms part of a GS catalytic multiprotein complex, and 2) Bgs4p-promoted cell-wall β-glucan alterations induce compensatory mechanisms from other Bgs subunits and (1,3)α-D-glucan synthase. Physiological localization studies showed that Bgs4p localizes to the growing ends, the medial ring and septum, and in each process of wall synthesis or remodeling that occurs during sexual differentiation: mating, zygote and spore formation, and spore germination. Bgs4p timing and requirements for proper positioning during cytokinesis and its localization pattern during spore maturation differ from those of Bgs1p. Bgs4p localizes overlapping the contractile ring once Bgs1p is present and a Calcofluor white-stained septum material is detected, suggesting that Bgs4p is involved in a late process of secondary or general septum synthesis. Unlike Bgs1p, Bgs4p needs the medial ring but not the Septation Initiation Network proteins to localize with the other septation components. Furthermore, Bgs4p localization depends on the polarity establishment proteins. Finally, F-actin is necessary for Bgs4p delocalization from and relocalization to the growing regions, but it is not needed for its stable maintenance at the growing sites, poles and septum. All these data show for the first time an essential role for a Bgs subunit in the synthesis of a (1,3)β-D-glucan necessary to preserve cell integrity when cell wall synthesis or repair are needed.

## INTRODUCTION

The fission yeast *Schizosaccharomyces pombe* provides an ideal model to study cell morphogenesis (Brunner and Nurse, 2000). The cells are cylindrical and grow by their ends in a polarized fashion (Chang and Peter, 2003; Hayles and Nurse, 2001). Genetic studies have identified many genes important for the different steps of cytokinesis, a process similar to that of animal cells, such as for the positioning and assembly of the actomyosin ring, the recruitment of actin patches to the medial ring, and the activation of ring contraction by a network of regulatory proteins referred to as the Septation Initiation Network (SIN), (Balasubramanian et al., 2004; Guertin et al., 2002; Krapp et al., 2004). Centripetal ring contraction and septum synthesis are perfectly coordinated, resulting in a three-layered septum structure between the membranes of both daughter cells that is composed of a middle disk structure called the primary septum, analogous to that of budding yeast (Schmidt et al., 2002), and flanked at both sides by the secondary septum. Once the septum has been completed, cell division proceeds by dissolution of the primary septum (Martin-Cuadrado et al., 2003).

The *S. pombe* cell wall is a well-organized structure consisting of an outer layer enriched in glycoproteins and an inner layer of carbohydrates, including (1,3)β-D-, (1,6)β-D- and (1,3)α-D-glucans (for a recent view see Duran and Perez, 2004; Perez and Ribas, 2004). (1,3)β-D-glucan is the major contributor to the cell wall framework. In situ localization studies (Humbel et al., 2001) have indicated that (1,6)β-D-branched (1,3)β-D-glucan is localized, forming filamentous structures all over the cell wall non-dense layer and throughout the septum; (1,6)β-D-glucan appears in the same cell wall non-dense layer and in the secondary septum, while linear (1,3)β-D-glucan is only present at the primary septum.

The enzyme complex involved in (1,3)β-D-glucan synthesis in yeast is (1,3)β-D-glucan synthase (GS). It is formed by at least two components: a regulatory and a catalytic subunit (Kang and Cabib, 1986; Ribas et al., 1991). The regulatory subunit is the GTPase Rho1p, which not only activates the GS (Arellano et al., 1996; Drgonova et al., 1996) but is also involved in other morphogenetic

processes, such as organization of the actin cytoskeleton and genesis of the growing regions (Arellano et al., 1999a; Cabib et al., 2001; Drgonova et al., 1999).

*S. pombe* contains four putative GS catalytic subunits named Bgs1p to Bgs4p. *bgs1*$^+$, *bgs2*$^+$ and *bgs3*$^+$ have been reported to be essential genes, at least for ascospore revival (Cortes et al., 2002; Liu et al., 2000; Liu et al., 1999; Martin et al., 2003; Martin et al., 2000), but nothing is known about *bgs4*$^+$. *bgs1*$^+$ was the first gene identified, initially named *cps1*$^+$. It was cloned by complementation of several mutants unable to assemble the division septum, and it was suggested to be involved in cytokinesis, polarity and in a septation checkpoint that coordinates cytokinesis and the cell cycle (Ishiguro et al., 1997; Le Goff et al., 1999; Liu et al., 1999). Recently, Bgs1p has been described to localize to the contractile ring and septum in a manner dependent on the actomyosin ring and SIN (Cortes et al., 2002; Liu et al., 2002), as well as to the growing poles and to other regions of cell wall synthesis during the sexual phase of the life cycle (Cortes et al., 2002). However, neither GS activity nor cell wall (1,3)β-D-glucan synthesis has been shown to depend on Bgs1p function. Therefore, the involvement of Bgs1p in (1,3)β-D-glucan synthesis remains to be clarified. *bgs2*$^+$ is not expressed in vegetative cells but is essential for proper spore wall maturation (Liu et al., 2000; Martin et al., 2000). *bgs3*$^+$ is also essential for vegetative cells and Bgs3p has also been shown to be localized to sites of cell wall growth. Similarly, *bgs3*$^+$ shut-off does not produce any apparent decrease in GS activity or cell wall (1,3)β-D-glucan, although the overall cell wall structure is altered (Martin et al., 2003). *Saccharomyces cerevisiae* contain two putative GS catalytic subunits, Fks1p and Fks2p, whose sequences share a high homology with Bgs proteins. *FKS1* and *FKS2* are redundant genes that are differentially expressed depending on the cycle or growth conditions. Single disruption of either *FKS1* or *FKS2* affords viable cells, but the double disruption is lethal (Mazur et al., 1995). A third *FKS* gene appears to be dispensable. Cell wall integrity is regulated by Rho GTPases and protein kinase C families (Arellano et al., 1999b). Alteration of these regulators dramatically affects GS activity, which in turn results in cell lysis. However, although the Bgs proteins code for putative GS catalytic subunits, neither Bgs1p nor Bgs3p elicits such a response, and indeed nothing is known about the GS catalytic subunit associated with this regulation that promotes such effects.

In this work, we characterized Bgs4p as the first Bgs subunit found to be part of the GS catalytic subunit. We show that the mutant *cwg1-1*, which displays reduced cell wall (1,3)β-D-glucan and GS catalytic subunit activity, is allelic to *bgs4*$^+$. We also show that Bgs4p is crucial for maintaining cell integrity, since its absence promotes cell lysis at the poles and septum. The data concerning *bgs4*$^+$ expression suggest that the GS catalytic subunit is a multiprotein complex. Bgs4p localizes to the growing poles, contractile ring and septum, and to each site of cell wall synthesis during the sexual phase of the life cycle. However, the requirements and timing of Bgs4p for proper positioning during septum formation as well as the localization pattern during spore maturation differ from those of Bgs1p. All the above data suggest that Bgs4p plays a role in each cell wall synthesis process of the *S. pombe* life cycle by synthesizing a (1,3)β-D-glucan that is essential for preserving cell integrity and reinforce its importance as an essential target for the design of specific antifungal drugs. In addition, the lytic phenotype observed during *bgs4*$^+$ shut-off may be biotechnologically useful as an efficient and controlled cell-free system for heterologous protein expression and purification (our priority patent application ES200401042; priority date April 30, 2004).

## MATERIALS AND METHODS

**Strains and Culture conditions.** The *S. pombe* strains used in this work are listed in Table 1. *bgs4*Δ strain 561 containing an integrated *GFP-bgs4*$^+$ copy was made by transforming strain 498 (*bgs4*Δ pJG33, *his3*$^+$ selection) with *Stu*I-cut pJG53 (*leu1*$^+$ selection, see below), which directs its integration at the *Stu*I site adjacent to *bgs4*Δ*::ura4*$^+$, at position -1320 of the *bgs4*$^+$ promoter sequence. The *GFP-bgs4*$^+$ and *bgs4::ura4*$^+$ sequences are separated by a pJK148 backbone. In order to eliminate pJG33, to analyze GFP-Bgs4p functionality, and to confirm that integration was in the *bgs4*$^+$ promoter sequence, this strain was crossed with strain 285 (Leu$^-$, Ura$^-$, His$^-$) and tetrad analysis was performed. Leu and Ura phenotypes always co-segregated 2+:2-. pJG33 was lost in most of the clones as result of the sporulation process. The *GFP-bgs4*$^+$ *bgs4*Δ strain obtained displayed a wild-type phenotype under all conditions tested and expressed GFP-Bgs4p at physiological level, from a single integrated *GFP-*

*bgs4*$^+$ gene under the control of its own promoter.

Standard complete yeast growth (YES), selective (EMM) supplemented with the appropriate amino acids (Alfa et al., 1993), and sporulation media (SPA) (Egel, 1984) have been described elsewhere. EMM-N is EMM (0.5% $NH_4Cl$) from which $NH_4Cl$ has been omitted. Stable sterile diploids for complementation analyses were obtained by mating mat2P-B102 and h$^-$ strains (Egel, 1984). The general procedures for yeast culture and genetic manipulations were carried out as described (Moreno et al., 1991). Latrunculin A (Lat A) was from Sigma and was used at 100 μM final concentration (from a stock solution of 10 mM in DMSO). Cell growth was monitored by measuring the $A_{600}$ of cell cultures in a Coleman Junior II spectrophotometer ($OD_{600}$ 0.1 = 1x10$^7$ cells/ml).

*Escherichia coli* strains DH5α and DH10B (Life Technologies) were used for routine propagation of plasmids (Sambrook and Russell, 2001), and CJ236 (Bio-Rad) was used for site-directed mutagenesis. Bacterial LB, 2xYT and TB media, supplemented with 100 μg/ml ampicillin or 50 μg/ml kanamycin, when appropriate, and standard transformation methods (Sambrook and Russell, 2001) have been described elsewhere.

**Plasmids and DNA techniques.** pJG1 (pAL-*bgs4*$^+$) is the 8.84 kb *Pst*I-*Nhe*I DNA fragment containing the *bgs4*$^+$ gene sequence from cosmid clone SPCC1840c (35 kb insert and kanamycin resistance selection, The *S. pombe* Genome Sequencing Project, Sanger Institute, UK) cloned into the *Pst*I-*Spe*I sites of *S. pombe* vector pAL-KS$^+$ (*S. pombe ars1*$^+$ and *S. cerevisiae LEU2* selection). pJG4 (pJK-*bgs4*$^+$) is the *Pst*I-*Nhe*I *bgs4*$^+$ fragment from SPCC1840c cloned into the *Pst*I-*Spe*I sites of the integrative plasmid pJK148 (*S. pombe leu1*$^+$ selection).

pJG9 is pJG1 with *Not*I from the multiple cloning site destroyed and with *Xho*I and *Pst*I sites inserted by site-directed mutagenesis just before the start codon and just after the TAG stop codon of *bgs4*$^+$, respectively. pJG17, pJG18 and pJG19 are pJR2-3XL, pJR2-41XL and pJR2-81XL (*S. cerevisiae LEU2* selection and 3X, 41X and 81X versions of thiamine-repressible *nmt1*$^+$ promoter, respectively) (Moreno et al., 2000) containing the *Xho*I-*Pst*I *bgs4*$^+$ ORF sequence from pJG9, respectively. pJG33 is pJR1-81XH (*S. pombe his3*$^+$ selection) (Moreno et al., 2000) with the *Xho*I-*Apa*I *bgs4*$^+$ ORF sequence

from pJG18. The resulting *S. pombe* strains *bgs4*Δ pJG18, pJG19 and pJG33 displayed a lytic phenotype after repressing the *nmt1*$^+$ promoter in the presence of thiamine.

pJR111 is pSK$^+$-*ura4*$^+$ (Moreno et al., 2000) with the 1.45 kb promoter and 1.0 kb terminator sequences of *bgs4*$^+$, amplified by PCR and cloned into *Apa*I-*Cla*I (5´ to *ura4*$^+$) and *Bam*HI-*Xba*I (3´to *ura4*$^+$), respectively. This plasmid was used for PCR amplification of the *bgs4*$^+$ deletion cassette, as described below.

pJG10 is pJG9 with a 9 bp insertion containing a *Not*I site just after the ATG initiation codon of the *bgs4*$^+$ ORF. pJG27 (pAL-*GFP-bgs4*$^+$, GFP inserted at aminoacid 2) is pJG10 cut with *Not*I and with the 0.74 kb *Not*I-*Not*I *GFP* fragment from pKS$^+$-*GFP* (GFP2-5, modified GFP sequence with changes S65T, V163A, I167T and S175G (Fernandez-Abalos et al., 1998)) inserted in-frame. GFP-Bgs4p from pJG27 proved to be non-functional since strain *bgs4*Δ pJG27 was not viable. Similarly, Bgs4p containing a C-terminal GFP fusion was not functional either. In order to obtain a functional GFP-Bgs4p fusion, the four most hydrophilic and N-terminal regions, as deduced from hydropathy analysis, were selected. Then, the aminoacids predicted to be at the boundaries between the secondary structures were chosen, and the 3xFLAG immunoreactive epitope was inserted in-frame at bases 85, 295, 694 and 970 (aminoacids 29, 99, 232 and 324) of the *bgs4*$^+$ sequence from pJG9. Only the plasmids with insertions at bases 85 and 970 expressed a functional *3xFLAG-bgs4*$^+$ fusion. pJG39 and pJG41 (pAL-*GFP-bgs4*$^+$, *GFP* at base 85 and 970, respectively) are pJG9 with a 9 bp *Not*I insertion at bases 85 and 970 of the *bg4*$^+$ ORF and with the *GFP* sequence inserted in-frame in the *Not*I site, respectively. Both pJG39 and pJG41 restored the wild-type phenotype to a *bgs4*Δ strain. pJG44 and pJG53 (pJK-*GFP-bgs4*$^+$, *GFP* at base 85 and 970, respectively) are the integrative plasmid pJG4 with the *Pst*I-*Bgl*II *bgs4*$^+$ sequence replaced by the *Pst*I-*Bgl*II *GFP-bgs4*$^+$ sequence from pJG39 and pJG41, respectively. pJG53, but not pJG44, expressed a fully functional fusion protein and was therefore selected to create the *GFP-bgs4*$^+$ *bgs4*Δ strains for Bgs4p localization studies at physiological level.

The sequences of native tetrameric DsRed (pDsRed2-1) and of the dimeric HcRed (pHcRed1-1) proteins (Clontech) were used to create an alternative fusion with the *bgs4*$^+$ sequence but none of these fusions resulted in a functional Bgs4p. Next, the sequence of the monomeric mutant form of DsRed

protein (*mRFP*) (Campbell et al., 2002) was used to create a functional RFP-Bgs4p fusion. pRSETB-mRFP1 contains the 678 bp ORF sequence of *mRFP1* cloned into *Bam*HI-*Eco*RI of pRSETB (Invitrogen). This plasmid was modified to insert two 9 bp *Not*I sites, after the ATG initiation codon and before the TAA stop codon, affording pJG84. This *mRFP Not*I-*Not*I sequence can be inserted in the same *Not*I sites as those used for *GFP* sequence. pJG52 is the integrative plasmid pJG4 with a 9 bp *Not*I site inserted at base 970 of *bgs4*$^+$. pJG87 is pJG52 with *Not*I from the multiple cloning site destroyed (*Xba*I-*Sac*II deletion) and with the *mRFP* sequence inserted in-frame in the *Not*I site of *bgs4*$^+$ at base 970. pJG101 is pJG87 with the two *Stu*I sites of the *mRFP* sequence destroyed, without changing the aminoacid sequence. The integrated *Stu*I-cut pJG101 plasmids expressed a functional fusion protein in a *bgs4*Δ strain and were therefore selected for localization studies.

*S. pombe* transformation was carried out using the LiAc method (Gietz et al., 1995). Other DNA manipulations were performed essentially as described (Moreno et al., 2000; Sambrook and Russell, 2001).

**Gene deletion.** *bgs4*$^+$ gene deletion was performed in the Leu$^-$ Ura$^-$ diploid strain 315. The 4.1 kb deletion cassette was generated by PCR amplification from pJR111. It eliminates the entire *bgs4*$^+$ coding sequence and contains 1.4 kb of the *bgs4*$^+$ promoter, the 1.76 kb *ura4*$^+$, and 1.0 kb of *bgs4*$^+$ terminator sequences. Correct deletion of the *bgs4*$^+$ ORF was confirmed by PCR analysis of both ends of both *bgs4*$^+$ and *bgs4*Δ*::ura4*$^+$ sequences, using combinations of oligonucleotides external and internal to the deletion fragment (data not shown). Tetrad analysis of sporulated *bgs4*$^+$/*bgs4*Δ diploids showed Bgs4p to be essential. Haploid *bgs4*Δ strains were obtained by random spore analysis of *bgs4*$^+$/*bgs4*Δ strains transformed with the *bgs4*$^+$-carrying plasmids pJG1, pJG17, pJG18 and pJG19, and selection of Leu$^+$ (*bgs4*$^+$ plasmids), Ura$^+$ (*bgs4*Δ), Ade$^-$ (haploidy marker) clones. Strain 498 *bgs4*Δ pJG33 (*his3*$^+$ selection) was obtained by genetic cross of strains *bgs4*Δ pJG1 and 285 (Leu$^-$ Ura$^-$ His$^-$) transformed with pJG33. Additional *bgs4*Δ strains were obtained by genetic cross of wild-type strain 285 and *bgs4*Δ pJG33 transformed with the corresponding plasmid.

**Enzyme preparation and (1,3)β-D-glucan synthase assay.** Cell extracts and GS assay were essentially as described (Cortes et al., 2002). Cell extracts were obtained from early-logarithmic phase cells grown in EMM as indicated for each case. Standard GS assay contained 15-25 μg protein of enzyme extract (3-5 mg protein/ml) in a total volume of 40 μl, and the reaction was incubated at 30°C for 60-90 minutes. All reactions were carried out in duplicate and the values were calculated from three independent cell cultures.

**Labeling and fractionation of cell wall polysaccharides**

$^{14}$C-glucose labeling and fractionation of cell wall polysaccharides were carried out essentially as described (Ishiguro et al., 1997). Exponentially growing cells were incubated as indicated in EMM supplemented with D-[U-$^{14}$C]glucose, as specified for each case of *bgs4*$^{+}$ shut-off (5 μCi/ml control cells and 9 μCi/ml shut-off cells) or overexpression induction (3 μCi/ml control cells and 4 μCi/ml overexpression cells), and they were collected at the indicated times. All determinations were carried out in duplicate, and the values for each strain were calculated from three independent experiments.

**Fluorescence microscopy.**

Cell colony and spore images were obtained directly from the growing plate with a Zeiss Axiophot microscope, a Plan-NEOFLUAR 40x/0.75 Ph2 objective, a RT Monochrome SPOT digital camera and SPOT V3.4.2 software (Diagnostic Instruments). For cell wall staining, early-logarithmic phase cells grown in YES or EMM liquid medium were concentrated and visualized directly by adding a solution of Calcofluor white (CW, 50 μg/ml final concentration), using the appropriate UV filter. For F-actin visualization, cells were fixed and stained with rhodamine-conjugated phalloidin, as described (Alfa et al., 1993). Nucleus and cell wall staining and direct GFP fluorescence visualization of early-logarithmic phase cells were essentially as described, suspending the cells in PBS containing 20 μg/ml CW and 10 μg/ml Hoechst (No. 33258, Sigma) (Cortes et al., 2002). Images were obtained with a Leica DM RXA fluorescence microscope as previously described (Cortes et al., 2002).

## RESULTS

### *bgs4*$^+$, *cwg1*$^+$ and *orb11*$^+$ are the same gene.

The gene coding for the fourth Bgs subunit, *bgs4*$^+$, has been found by the *S. pombe* Genome Sequencing Project (SPCC1840.02c), and consists of an open reading frame of 5,868 nucleotides; it encodes a predicted membrane protein of 1,955 aminoacids with a molecular weight of 225kDa. Bgs4p shows sequence identity ranging from 53 to 59% with other Bgs proteins and from 49% to 57% with *S. cerevisiae* Fks proteins. The cosmid clone that contains *bgs4*$^+$ is located close to and between the cosmids that contain the *ppe1*$^+$ (= *ppx1*$^+$ / *esp1*$^+$) and *ade5*$^+$ genes.

Interestingly, a previous search for *S. pombe* mutants affected in cell wall (1,3)β-D-glucan biosynthesis led to the characterization of the *cwg1-1* mutant (Ribas et al., 1991). This mutant showed a rounded thermosensitive lethal phenotype, accompanied by a considerable reduction in cell wall β-glucan (25% wild type amount) and GS activity (25% wild type activity); this defect was associated with the insoluble catalytic fraction of the enzyme. Unfortunately, cloning of the corresponding *cwg1*$^+$ gene using different gene libraries was unsuccessful. By genetic analysis, *cwg1*$^+$ was mapped to the same region as *bgs4*$^+$: on the right arm of chromosome III, linked to and mapping between *ppe1*$^+$ and *ade5*$^+$. Therefore, the close location of *bgs4*$^+$ and *cwg1*$^+$ and the hypothetical involvement of both gene products as part of the GS catalytic subunit suggest that *bgs4*$^+$ and *cwg1*$^+$ could be the same gene.

To test this notion, the *bgs4*$^+$ gene was cloned from the cosmid clone SPCC1840c and the plasmid obtained, pAL-*bgs4*$^+$ (pJG1), was used to transform the *cwg1-1* mutant strain. It was found that *bgs4*$^+$ was able to suppress all the *cwg1-1* defects: 1) the lethal phenotype at 37°C (Figure 1A), 2) the spherical morphology prior to lysis (data not shown), 3) the increased cell wall fluorescence in the presence of the fluorochrome Calcofluor white (CW), which preferentially binds cell wall material (data not shown), and 4) the low (25%) in vitro GS activity (Figure 1B) and in vivo cell wall β-glucan content. In addition, the same suppression of all the phenotypes was obtained with another mutant allele: *cwg1-2* (Perez and Ribas, 2004) (data not shown). Moreover, genetic cross between

*bgs4*$^+$*:leu1*$^+$ *leu1-32* and *cwg1-1 leu1-32* strains showed no recombination (98 PD: 0 T: 0 NPD) between *bgs4*$^+$ (Leu$^+$ phenotype) and *cwg1-1* (lytic phenotype) markers. This tight linkage (<0.51 cM) suggested that *bgs4*$^+$ and *cwg1*$^+$ are the same gene. This was finally corroborated by complementation analysis in diploid strains. The *cwg1-1* mutant phenotype was recessive in heterozygosis, as described (Ribas et al., 1991), but the heterozygous *cwg1-1*/*bgs4*Δ strain displayed the same thermosensitive phenotype as the homozygous *cwg1-1*/*cwg1-1* strain (Figure 1C). This proves that *cwg1*$^+$ and *bgs4*$^+$ are the same gene.

Genetic analysis revealed a tight linkage between *cwg1-1* and the thermosensitive mutant *orb11-59*, which has been described as rounded and showing a complete loss of cell polarity (Verde et al., 1995). Like *cwg1-1*, *orb11-59* defects were not suppressed by multicopy expression of any of the three homologous genes *bgs1*$^+$, *bgs2*$^+$ or *bgs3*$^+$ (data not shown). In contrast, both multicopy and integrated *bgs4*$^+$ expression suppressed the lethal and morphological phenotypes of the *orb11-59* strain (Figure 1D), indicating that *bgs4*$^+$, *cwg1*$^+$ and *orb11*$^+$ are the same gene.

**Bgs4p is essential for cell integrity during both cytokinesis and polarized growth.**

In order to study the effect produced by the absence of Bgs4p in the cell, we constructed a heterozygous diploid strain, *bgs4*$^+$/*bgs4*Δ, by replacing the entire *bgs4*$^+$ open reading frame with the *ura4*$^+$ gene (see Methods). Tetrad analysis of sporulated diploids showed that only the two Ura$^-$ (*bgs4*$^+$) clones of each tetrad were viable and sorbitol was unable to rescue the viability of the *bgs4*Δ spores (Figure 2A). Therefore, *bgs4*$^+$ is essential at least during spore germination, as reported for *bgs1*$^+$ and *bgs3*$^+$ (Cortes et al., 2002; Liu et al., 1999; Martin et al., 2003). Microscopic observation revealed that *bgs4*Δ spores were able to germinate but that they lysed before the first round of cell division (Figure 2A). In contrast, *bgs1*Δ spores were able to germinate, producing enlarged and multiseptated cells that eventually died (data not shown), and *bgs3*Δ spores germinated and divided several times, producing small groups of rounded cells (Martin et al., 2003).

In order to analyze the effect of the absence of *bgs4*$^+$, it was expressed under the control of the 41X (medium) and 81X (low) versions of the thiamine-regulatable *nmt1*$^+$ promoter (see Methods). Viable

*bgs4*Δ cells were obtained only when the 41X or 81X promoter was induced (Figure 2B). In both cases the cells had a growth rate and morphology similar to wild-type cells. According to the different expression levels of these *nmt1*$^+$ promoters (Moreno et al., 2000), *S. pombe* cells can support at least a 50-fold difference in *bgs4*$^+$ expression. *bgs4*$^+$ shut-off arrested cell growth, this occurring earlier in the p81X-*bgs4*$^+$ strain (data not shown). After 14 hours of *bgs4*$^+$ repression, the cells stopped growing (Figure 2B), and unlike the *cwg1-1*, *cwg1-2* and *orb11-59* mutant alleles, osmotic stabilization only partially protected the cells, delaying the arrest of growth to 17 hours and maintaining a residual growth (Figure 2B).

Morphological observations revealed that *bgs4*$^+$ repression promoted cell lysis and the release of cytoplasmic material to the regions of cell wall synthesis, either the poles or the septum (Figure 2C). Lysis at the septum appeared earlier and was more abundant than at the poles: 15% at 14-15 hours and increasing up to 70-80% at 21-23 hours after *bgs4*$^+$ shut-off (data not shown). Initially, the lysis occurred at the border between the septum and cell wall of one of the daughter cells, giving rise to one dead cell whose cell wall remained attached on one side to the live cell; this probably retained most of the previously formed cell wall and hence had a better chance of survival. At longer times, lysis occurred at both sides of the septum (Figure 2C), resulting in the death of both cells. Lysis at the poles usually appeared after 17 hours and increased up to 21-23 hours of shut-off, representing around 10% of the cells. Sorbitol delayed lysis at the poles but not that at the septum (data not shown), and the surviving cells had a healthier aspect and were able to maintain a slow increase in cell density (Figure 2B), although eventually they died. These results suggest that the function of Bgs4p at the cell wall-septum boundary is more critical than that at the poles. A small population was able to survive *bgs4*$^+$ shut-off, giving rise to stable but sickly spherical revertants (data not shown), probably due to cell wall compensatory mechanisms (see Discussion). Actin staining during shut-off showed that after 8 hours actin patches began to appear dispersed throughout the cytoplasm, disappearing from or being present in lower amounts at both the septum and poles. However, the contractile actomyosin ring remained stable, even at the time of cell lysis (Figure 2E).

Analysis of in vitro GS activity during *bgs4*$^+$ shut-off and before cell lysis revealed a dramatic decrease in activity (Figure 2D), similar to that reported for the *bgs4*$^+$ mutant allele *cwg1-1* (Ribas et al., 1991). Next, the cell wall composition was analyzed immediately before cell lysis had begun. Surprisingly, the amount of cell wall did not decrease; instead, it rose from 33 to 43% and this increase was only due to α-glucan, suggesting an in vivo compensatory mechanism (Table 2). The increase in α-glucan and total cell wall was attenuated in the presence of sorbitol (Table 2) and was enhanced when the cells were grown at 37°C (24% α-glucan and 50% cell wall, data not shown). Contrary to the GS activity, cell wall β-glucan did not decrease, probably due to a compensatory mechanism (see Discussion). All these data indicate that Bgs4p is critical for maintaining cell integrity at any site where cell wall growth takes place.

**_bgs4_$^+$ overexpression causes defects in cell wall integrity.**

*bgs4*Δ p3X-*bgs4*$^+$ cells grow normally under repressed conditions (expression is 5-fold higher than with the induced 81X promoter, (Moreno et al., 2000)). However, *bgs4*$^+$ overexpression promoted the arrest of cell growth 16-18 hours after induction and sorbitol merely delayed it to 20 hours and permitted a residual growth (Figure 3A). Contrary to *bgs4*$^+$ shut-off, *bgs4*$^+$-overexpressing cells were viable for several days, 80% and 70% of viable cells remaining after 15 and 30 hours of overexpression, respectively (data not shown). The cells maintained a slow growth pattern and increased their heterogeneous phenotype of rounded and elongated cells, some becoming refringent and containing aberrant depositions of CW-stained cell wall material (Figure 3B). Actin staining showed that after 24 hours of overexpression the actin patches were delocalized throughout the cytoplasm in the rounded cells, disappearing mainly from the poles but still remaining localized to the septum to some extent (Figure 3C).

Unexpectedly, GS activity decreased during *bgs4*$^+$ overexpression. This activity was only 65% at 15 hours, when the cells still had no apparent phenotype, and decreased dramatically to 30% at 30 hours (Figure 3D). This suggests that the GS catalytic subunit may be composed of a multiprotein complex rather than by Bgs4p alone (see Discussion). Cell wall analysis during *bgs4*$^+$ overexpression revealed

an increase in cell wall due to α-glucan, while β-glucan was not affected (Table 3), suggesting that - as for its shut-off - *bgs4*$^{+}$ overexpression promotes the activation of cell wall compensatory mechanisms.

**Bgs4p localizes to one or both poles during cell growth and to the contractile ring and septum during cytokinesis.**

Neither a C-terminal nor a N-terminal GFP-Bgs4p fusion was able to maintain Bgs4p functional. Similarly, other fusions with GFP inserted in the N-terminal region of Bgs4p were not functional either (see Methods). Only GFP-Bgs4p with GFP inserted at aminoacid 324 completely restored the wild-type phenotype to a *bgs4*Δ strain and also showed localized the GFP fluorescence. Therefore, this *GFP-bgs4*$^{+}$ *bgs4*Δ strain (GFP at aminoacid 324, integrated single copy, own promoter and absence of original *bgs4*$^{+}$ gene) was chosen for Bgs4p localization studies.

The cells were visualized by GFP fluorescence to detect Bgs4p and by CW staining, which preferentially binds to cell wall material, probably (1,3)β-D-glucan, of the septum and growing zones. CW staining revealed the fluorescence at the single growing pole during monopolar growth, at both poles during bipolar growth, and at the septum during cytokinesis. Bgs4p was found to localize to the growing ends and septum along the mitotic cycle, overlapping the CW staining (Figure 4A).

Initially, some dividing cells were able to separate before resuming growth, Bgs4p appearing at the new pole formed after septum degradation. When cell growth began, Bgs4p accumulated at the growing old end. During bipolar growth, Bgs4p also localized to the opposite pole. Finally, after a CW-stained septum material had become visible, the GFP disappeared from both poles and localized to the middle of the cell, concentrating as two faint dots at both sides of the emerging septum. Then, the GFP moved to the tip of the growing septum, concentrating in a narrow ring that moved centripetally with the edge of the growing septum. The GFP signal was stronger where the ring was intersected by the focal plane. An apparent signal remained along the invaginated membrane where new cell wall material had been synthesized (Figure 4B). After the septum wall had been completed, the GFP appeared in two separated bands. During cell division, Bgs4p remained at both sides of the septum until the two daughter cells were ready to or already had separated, then changing its

localization to the old end of each daughter cell, which then initiated monopolar growth (Figure 4A,B).

Bgs1p has also been described to localize to septum and poles (Cortes et al., 2002) but its localization pattern during septation seemed to differ in some aspects from that of Bgs4p. Therefore, GFP-Bgs1p and GFP-Bgs4p were compared as regards their localization and displacement from the tips to the medial ring during mitosis (Figure 4C). Bgs1p and Bgs4p localized to both cell ends until the end of anaphase, when nuclear division had been completed. When the nuclei were migrating to the cell poles Bgs1p, but not Bgs4p, disappeared from the poles, appearing as two GFP dots at the middle of the cell. Then, after the nuclei had reached the cell poles, two CW-stained septum dots appeared overlapping the bright GFP-Bgs1p signals. Simultaneously, GFP-Bgs4p began to disappear from the poles and to concentrate diffusely in the middle of the cell. Next, when the septum and GFP-Bgs1p dots were intense, GFP-bgs4p condensed at both sides of the septum. Finally, GFP-Bgs4p moved towards and appeared concentrated at the end of the growing septum, overlapping GFP-Bgs1p (Figure 4C). Therefore, Bgs1p moves earlier than Bgs4p to the division site during mitosis, appearing before any septum material can be detected, while Bgs4p appears later, after the septum has become visible.

**Bgs4p localization during septation depends on the medial ring but not on the Septation Initiation Network.**

In order to study the requirements of Bgs4p localization during septation, several septation mutants were generated in a *GFP-bgs4*$^{+}$ *bgs4*Δ background and GFP-Bgs4p localization was analyzed. The anillin-like Mid1p is located to the middle zone and is essential for correct positioning of the medial ring (Bahler et al., 1998; Sohrmann et al., 1996). The *mid1* mutants show the actomyosin ring and septum positioned at random locations and angles (Chang et al., 1996), coincident with the localization of Bgs1p and with the CW-stained septum material (Cortes et al., 2002). Initially, Bgs4p positioning coincided with the altered ring and septa (Figure 5), suggesting that Bgs4p localization is not dependent on Mid1p and that it can interact with the rest of the septation components and localizes to the abnormally positioned septa. However, cells with the aggravated mutant phenotype displayed

aberrant CW-stained septum material, previously shown to be coincident with Bgs1p localization (Cortes et al., 2002), but that did not necessarily overlap Bgs4p localization (compare arrowhead and arrow positions in *mid1-366* cells in Figure 5). Considering that Bgs4p would remain functional as in wild-type *bgs4*Δ cells, this result suggests that Bgs4p is responsible for the synthesis of a (1,3)β-D-glucan not stained by CW and, reciprocally, that CW detects a cell wall component, probably glucan, synthesized by other proteins, such as Bgs1p.

The profilin Cdc3p is essential for the assembly of the medial ring actin filaments (Balasubramanian et al., 1994; Chang et al., 1996). *cdc3-6* mutants show defects in septum formation but not in cell elongation and they accumulate CW-stained cell wall material at the site of septum formation (Nurse et al., 1976). Bgs4p was detected at the poles and/or overlapping with many of the cell wall structures synthesized at the middle of the cell (Figure 5). The PCH family Cdc15p is essential for cell division and the mutants display impaired actin ring formation or form unstable ring structures, although they are not impaired in cell elongation (Chang et al., 1996; Fankhauser et al., 1995). In the *cdc15-140* mutant, Bgs4p was detected either dispersed in the cytoplasm or at the cell poles but not at the middle of the cell. Also, the mutant sometimes showed thick or diffuse aberrant cell wall structures resembling the septa but in which Bgs4p was never present (Figure 5). Cdc16p forms a two-component GAP for Spg1p GTPase that is required for negative regulation of septum formation (Cerutti and Simanis, 1999; Furge et al., 1998). The *cdc16-116* mutants formed multiple septa due to their failure to turn off septation. Bgs4p was located at the poles and at many of the multiple septa (Figure 5). In sum, these data indicate that the contractile ring is necessary for Bgs4p localization to the middle of the cell.

Next, we wondered whether the SIN proteins are necessary for Bgs4p displacement from the tips to the medial ring during mitosis or for its stable localization to the medial ring. To check this, CW and nucleus staining, and GFP were analyzed simultaneously in the same cells. The SIN proteins Cdc11p and Cdc14p are essential for septum formation (Guertin et al., 2000; Krapp et al., 2004; Krapp et al., 2001). The *cdc11-119* and *cdc14-118* mutants have cytokinesis blocked but assemble actomyosin rings during mitosis and accumulate actin patches at the cell ends during interphase. In these mutants,

GFP-Bgs4p localized to the poles, coinciding with cell growth (Figure 5 and data not shown). Some *cdc14-118* cells exhibited CW-stained septum structures (shown by arrowheads in *cdc14-118* cells in Figure 5), formed before they expressed the thermosensitive phenotype. Analysis of *cdc14-118* cells at different incubation times (3 to 6 hours) at the restrictive temperature, which results in cells containing 2, 4 and 8 nuclei, elicited no change in the amount of cells with partial septum structures and absence of complete septa in all the cases. This indicates that these septum structures are inactive and never progress to complete the corresponding septum. Analysis of both mutants revealed that Bgs4p never relocated to the medial ring in cells lacking a partial septum. However, the number of cells with no partial septum showing internalized Bgs4p was higher than that observed in wild-type cells (data not shown), suggesting that contrary to the requirements of Bgs1p (Cortes et al., 2002), SIN signaling is not necessary for post-anaphase Bgs4p displacement from the tips to the middle of the cell. Additionally, when a partial septum structure was present, Bgs4p could be found at the poles and absent from the medial ring, or located to the contractile ring (shown by arrows in *cdc14-118* cells in Figure 5) and absent from the poles, or at both sites simultaneously (Figure 5). Therefore, SIN proteins are dispensable for Bgs4p localization to the medial ring when a partial septum structure is present.

**Bgs4p localization depends on polarity establishment proteins.**

Bgs4p was localized to the poles during both monopolar and bipolar growth. The *tea1-1* and *tea2-1* mutants do not recognize the old end and activate a new incorrectly positioned growing site due to a failure to establish polarized growth along the long axis of the cell (Browning et al., 2003; Sawin and Snaith, 2004; Verde et al., 1995). In these mutants, Bgs4p appeared localized to the incorrect new growing tips or to the mislocalized septum. Similarly, the double mutant *tea2-1 cdc11-119* activates several new growing ends in which Bgs4p was always present (Figure 6A). Therefore, Bgs4p - like Bgs1p and Bgs3p (Cortes et al., 2002; Martin et al., 2003) - remains polarized to the growing sites independently of its mislocalization due to a failure of the polarity proteins to establish the correct growing ends.

**The actin cytoskeleton is necessary for Bgs4p delocalization and relocalization but not for its maintenance at the growing sites.**

F-actin localizes to either the growing tips or the dividing medial region, playing a role in cell wall synthesis and polarized growth (Kobori et al., 1989; Marks et al., 1986). Actin coincides with Bgs4p localization along the cell cycle and we were therefore prompted to analyze whether the actin cytoskeleton is involved in correct Bgs4p localization as well. The actin mutant *cps8-188* shows rounded and enlarged cells in which the actin remains polymerized but randomly distributed and the middle ring is absent (Ishiguro and Kobayashi, 1996). Bgs4p localization extended from the septum and poles along the plasma membrane all around the cell (Figure 6B). Intermediate phenotypes showed cells with aberrant contractile ring structures, in which Bgs4p localized simultaneously to the septum, poles, and regions of aberrant cell wall synthesis (data not shown). The profilin mutant *cdc3-6* presents a terminal phenotype reflecting the absence of F-actin structures. The *cdc3-6* cells contain aberrant septa and cell wall structures as a result of a previous intermediate phenotype in which Bgs4p was absent, appearing delocalized inside the cell as a low GFP background (data not shown). Thus, Bgs4p localization depends on the polymerized F-actin cytoskeleton and its specific localization to regions of active cell-wall synthesis depends on the correct localization of polymerized F-actin, as reported for Bgs1p, Fks1p and the putative (1,3)α-D-glucan synthase Ags1p/Mok1p (Cortes et al., 2002; Katayama et al., 1999; Utsugi et al., 2002).

We next analyzed in greater detail the role of F-actin in Bgs4p localization. We used *bgs4Δ RFP-bgs4*$^{+}$ *crn1*$^{+}$*-GFP* cells to analyze - in the same cells - Bgs4p localization by RFP fluorescence and F-actin patches localization by GFP fluorescence of the coronin homologue Crn1p, a protein associated with and used as a marker for F-actin patches and cables (Pelham and Chang, 2002; Pelham and Chang, 2001). First, we wondered if the F-actin cytoskeleton is necessary for stable Bgs4p maintenance at the growing regions. The cells were treated for 15 minutes with latrunculin A (Lat A), which prevents actin polymerization. As control, cells were incubated with DMSO, showing no effect on Bgs4p or actin patches localization (data not shown). Lat A-treated cells displayed the absence of polymerized actin patches, with the GFP fluorescence distributed uniformly in the cytoplasm, while

Bgs4p remained localized, indistinguishable from control cells (Figure 7A). A longer Lat A treatment of 30 minutes produced the same effect on Bgs4p and actin localization, but the cell recovery time required to relocalize both Bgs4p and F-actin increased up to 2 hours (data not shown). This indicates that F-actin is not needed for stable Bgs4p maintenance to the medial ring and poles. Then, Lat A was removed to analyze the recovery of actin patches. At 30 minutes of Lat A wash out, the actin patches reappeared and were randomly localized, while by contrast, Bgs4p had lost its polarization and appeared transiently delocalized inside the cell (Figure 7A). At 1 hour, the actin patches were partially localized and Bgs4p had relocalized to the growing sites. At 3 hours, both the actin patches and Bgs4p localization were fully recovered (Figure 7A). Next, we speculated whether the observed transitory Bgs4p delocalization and relocalization might be due to the transient random distribution of the repolymerized actin patches. Initially, the cells were exposed to stress conditions (2 hours at high temperature and absence of nitrogen). Under these conditions, the F-actin patches appeared randomly localized and partially depolymerized and Bgs4p was completely delocalized inside the cell (Figure 7B). Then, the cells were transferred to fresh YES complete medium, either in the presence or absence of Lat A. In the presence of Lat A, actin appeared depolymerized in the cytoplasm and Bgs4p was unable to relocalize to the growing zones for at least 2 hours. After 1 hour in the absence of Lat A, the control cells already displayed a few actin patches localized to the growing regions and part of Bgs4p appeared relocalized. At 2 hours, F-actin and Bgs4p appeared completely relocalized to the growing sites (Figure 7B). Therefore, the F-actin cytoskeleton is necessary for Bgs4p repolarization to the growing sites. In a third experiment, the cells were treated with Lat A as in Figure 7A to depolymerize the F- actin, but maintaining Bgs4p polarized. Then, the cells were exposed to stress conditions in either the presence or absence of Lat A (Figure 7C). In the presence of Lat A, actin remained depolymerized and Bgs4p remained polarized for at least 3 hours. In the control cells (absence of Lat A), it was observed that at 1 hour some actin had repolymerized as random actin patches and Bgs4p appeared delocalized inside the cell; this effect persisted for at least 3 hours (Figure 7C). Hence, the F-actin cytoskeleton is also needed for Bgs4p delocalization from the growing zones.

**Bgs4p is also localized to the growing zones during mating, spore wall formation and spore**

**germination.**

Bgs4p plays a major role in cell wall synthesis during vegetative growth and is present at each site where growth takes place. Therefore, we wondered if Bgs4p might also be present at the cell wall growth sites during the sexual phase of the life cycle in a homothallic *bgs4*Δ *GFP-bgs4*$^{+}$ h$^{90}$ strain. Initially, Bgs4p appeared localized in only one of both mating cells. Then, the mating partner responded by forming a mating projection to which Bgs4p localized (Figure 8). The cell walls of both cells fused and Bgs4p localized to the contact region that separates the cells. When the contact region had disappeared, Bgs4p remained as a wide band in the neck between both cells. Later, it disappeared from the neck membrane and began to fill in the whole cytoplasm, but not the fused nucleus, with a uniform fluorescence that persisted during the process of meiosis. Contrary to Bgs1p, Bgs4 never appeared inside or associated with the membranes of the oval-shaped prespores. Instead, it remained as a bright and uniform fluorescence in the cytoplasm and around the prespore. Although the prespores were perfectly distinguishable at phase contrast microscopy (data not shown), CW staining only revealed the zygote shape. Following this, Bgs4p fluorescence decreased transiently and reappeared as bright patches close to or around the spore wall. CW began to stain the spores, probably due to the maturation of the prespore wall to become a spore. Finally, Bgs4p fluorescence gradually disappeared, remaining only localized to the spore periphery and as faint patches inside the mature spores (Figure 8). In sum, these observations suggest Bgs4p may cooperate to form the mating projection and to protect the cell from an excess of cell wall degradation during cell fusion. In addition, Bgs4p may play a specific role in both prespore and spore wall synthesis.

We were interested in analyzing whether the initial asymmetry observed for the appearance of Bgs4p in the mating projections was related to a specific mating type. To do so, we analyzed the appearance of Bgs4p in the mating projections along the mating process of strains h$^{+}$ *GFP-bgs4*$^{+}$ *bgs4*Δ x h$^{-}$ *RFP-bgs4*$^{+}$ *bgs4*Δ and h$^{+}$ *RFP-bgs4*$^{+}$ *bgs4*Δ x h$^{-}$ *GFP-bgs4*$^{+}$ *bgs4*Δ (Figure 9). Initially, Bgs4p was found delocalized inside the cells. Then, both GFP- and RFP-Bgs4p began to appear localized in some cells of both h$^{+}$ strains (see arrowheads in Figure 9), while no h$^{-}$ cell showed localized Bgs4p. Following this, the amount of h$^{+}$ cells with localized GFP- or RFP-Bgs4p increased, and all the h$^{-}$ cells continued

displaying delocalized Bgs4p. One hour after the appearance of polarized Bgs4p in $h^+$ cells, some $h^-$ cells showed the first localized GFP- or RFP-Bgs4p (see arrows in Figure 9). Finally, the number of cells with localized Bgs4p increased to a similar extent in both mating types and the first zygotes appeared (Figure 9). Therefore, during the mating progression Bgs4p appears localized first in P ($h^+$) cells and later in M ($h^-$) cells, in agreement with the reported formation of mating projections in response to pheromones during the mating process (Nielsen and Davey, 1995).

Analysis of the localization of *bgs4*Δ *GFP-bgs4*$^+$ $h^{90}$ spores showed that Bgs4p might also be involved in the germination process (Figure 10). The spores were released by spontaneous lysis of the asci in the absence of any enzymatic treatment that might alter spore wall or Bgs4p localization. First, during isotropic spore growth Bgs4p fluorescence increased uniformly inside the spore, and more weakly all around the periphery. Then, the internal fluorescence disappeared and Bgs4p concentrated to the place where polarized growth began. CW stained the site of polarized growth, as in vegetative cells, and Bgs4p was localized to this growing pole. Next, Bgs4p reorganized to the middle of the cell, localizing to the medial ring and septum until the first cell was ready to separate. Finally, Bgs4p localized to the old end of the new cell but remained at the septation pole of the spore (Figure 10), probably because growth will resume only at this pole, with a vegetative cell structure.

## DISCUSSION

The fission yeast is an attractive morphogenetic model for understanding how fungi, and cells in general, regulate their polarized growth (Chang and Peter, 2003; Hayles and Nurse, 2001) and cytokinesis along the cell cycle (Balasubramanian et al., 2004; Guertin et al., 2002; Krapp et al., 2004). However, little is known about how fission yeast synthesizes and regulates its cell wall components during these processes; in particular (1,3)β-D-glucan as the main structural polysaccharide. *S. pombe* contains four putative GS catalytic subunits, although their involvement in (1,3)β-D-glucan synthesis has not yet been elucidated.

Here we cloned *bgs4*$^+$ and we show that it is the only *bgs* gene found to be essential to maintain cell

integrity during both cytokinesis and polarized growth. Also, Bgs4p is the first subunit directly involved as part of the GS catalytic subunit. First, *bgs4*$^{+}$ is the only gene of this family that has mutant alleles (*cwg1-1* and *cwg1-2*) with a specific reduction in cell wall (1,3)β-D-glucan and GS activity, the latter due to a defect in the catalytic subunit (Perez and Ribas, 2004; Ribas et al., 1991). Second, *bgs4*$^{+}$ shut-off promotes specific cell lysis at the growing regions, poles and septum; this is accompanied by a dramatic decrease in GS activity. A similar lysis occurred in germinating *bgs4*Δ spores, highlighting the importance of Bgs4p during spore germination. The specific localization of Bgs4p to the areas of active cell wall synthesis is consistent with these observations.

The predominant *bgs4*$^{+}$ shut-off phenotype is that of lysis at the already synthesized septum at the beginning of cell division, suggesting that the function of Bgs4p is not only essential for cell wall growth but also for cell wall repair, compensating an excess of septum wall degradation during cytokinesis.

The three mutants described for Bgs1p show similar septation defects (Ishiguro et al., 1997; Le Goff et al., 1999; Liu et al., 1999) but none of them show a defect in cell wall (1,3)β-D-glucan or GS activity, although the mutant phenotype, homology with Fks proteins, and Bgs1p localization have served to propose that this subunit would be responsible for the synthesis of a linear (1,3)β-D-glucan from the primary septum and growing poles (Cortes et al., 2002). Nonetheless, the true functions of Bgs1p remain obscure. No *bgs3* mutant has been described and *bgs3*$^{+}$ shut-off does not show any relationship with (1,3)β-D-glucan synthesis, measured as cell wall composition or enzymatic activity (Martin et al., 2003). Also, the *S. cerevisiae* homologue *FKS1* has been described from different mutant alleles, all of them either unrelated (Eng et al., 1994; Garrett-Engele et al., 1995; Ram et al., 1995) or indirectly related to GS activity owing to their resistance to the specific GS inhibitors papulacandin and echinocandin (Castro et al., 1995; Douglas et al., 1994). Fks1p has been implicated in GS activity because some of these mutants showed a reduction in GS or a general reduction in cell wall β-glucan and because partial purification of the GS membrane enzyme showed Fks1p to be present among the enriched proteins of the extract (Inoue et al., 1995). Conversely, different Fks1p mutations displayed a simultaneous reduction or increase in both cell wall (1,3)β and (1,6)β-D-glucan, and specific (1,6)β-D-

glucan mutants exhibited a decrease in GS activity similar to that of the *fks1*Δ mutant (Dijkgraaf et al., 2002). In addition, although the *fks1*Δ *fks2*Δ double mutant is lethal, no cell lysis at the growing regions or release of cytoplasmic material due to a defect in cell wall integrity have been described. Additionally, the *S. cerevisiae* Fks3p homologue is not essential and has no known function. In sum, Bgs4p is the first subunit that shows a direct in vivo involvement in cell wall (1,3)β-D-glucan synthesis and GS activity, detected by its mutants and shut-off phenotypes, as well as in the control of cell structure and integrity.

Contrary to the *cwg1-1* mutant allele, *bgs4*$^{+}$ shut-off did not elicit a decrease in cell wall (1,3)β-D-glucan, suggesting a compensatory mechanism that activates other Bgs subunits. In fact, this is consistent with the appearance of stable *bgs4*Δ revertants and with the considerable increase in at least GFP-Bgs1p during *bgs4*$^{+}$ shut-off (our unpublished results). The absence of Bgs4p would be necessary to activate this compensatory mechanism, since the presence of a partially non-functional protein in *cwg1* mutants did not display it. A similar mechanism might also be induced during *bgs3*$^{+}$ shut-off (Martin et al., 2003) but, unlike *bgs4*$^{+}$ shut-off, there is no decrease in GS activity, suggesting that Bgs4p is the main agent responsible for the in vitro-detected GS activity, as reported for *S. cerevisiae* Chs1p and chitin synthase activity (Roncero, 2002). Alternatively, the difference in cell wall β-glucan levels detected between the *cwg1-1* mutant and *bgs4*$^{+}$ shut-off could be due to a cumulative defect in the former that cannot be detected with a restricted but lethal defect produced by the absence of Bgs4p. In the case of Bgs1p, and contrary to the *cwg1-1* mutant, the *cps1-12* mutant did not show any decrease in GS or cell wall β-glucan. This is consistent with the idea of Bgs1p being responsible for the synthesis of a minor linear (1,3)β-D-glucan of the primary septum and nascent cell wall (Cortes et al., 2002).

We found that *S. pombe* also induces a stronger and more general compensatory mechanism in response to cell wall alterations and stress by increasing (1,3)α-glucan synthesis. This has been observed during *bgs4* shut-off or overexpression, *bgs3*$^{+}$ shut-off, expression of *cwg1-1* or *cps1-12* mutant phenotypes (Ishiguro et al., 1997; Martin et al., 2003; Ribas et al., 1991) and *bgs1*$^{+}$ shut-off or overexpression (our unpublished results).

*bgs4*$^{+}$ overexpression did not increase cell wall β-glucan or GS activity. Instead, it resulted in a considerable decrease in GS activity. The same result has been described for *bgs3*$^{+}$ (Martin et al., 2003). This effect is opposite to that observed when the single regulatory subunit Rho1p is overexpressed (Arellano et al., 1996) or with Ags1p/Mok1p overexpression and an increase in cell wall α-glucan (Katayama et al., 1999). It is unlikely this would be due to limiting concentrations of the Rho1p regulatory subunit, because in that case it would promote neither an increase nor a decrease in GS activity. This suggests that Bgs4p forms part of a multiprotein complex that constitutes the GS catalytic subunit. Thus, overproducing only Bgs4p would result in multiple partial complexes and a decrease in the enzymatic activity. Regarding its shut-off, cell wall (1,3)β-D-glucan would not decrease due to a compensatory mechanism from other Bgs proteins. Additional studies will be necessary to characterize the (1,3)β-D-glucan synthase catalytic components and the mechanism by which they and the Bgs proteins interact with each other.

For Bgs4p localization studies, we attempted to mimic the Bgs4p physiological state: an integrated single copy gene, its own promoter and the wild-type phenotype in a *bgs4*Δ background. The conformation of Bgs4p seems to be different or less stable than that of Bgs1p and Bgs3p, since the N-terminal GFP fusion is functional with Bgs1p and Bgs3p but not with Bgs4p. As reported for Bgs1p and Fks1p (Cortes et al., 2002; Delley and Hall, 1999), the localization of Bgs4p is very unstable and extremely sensitive to cell wall stress, mainly at the poles, but less so at the septum, and more stable at the contractile ring. Bgs4p localization during septation was delayed with respect to that of Bgs1p, supporting the idea that Bgs1p would synthesize a (1,3)β-D-glucan of the primary septum (Cortes et al., 2002) and that Bgs4p would synthesize a major (1,3)β-D-glucan present in the secondary septum in a process that is delayed but overlapping with primary septum synthesis. In *S. cerevisiae*, the primary septum is made of chitin. *S. pombe* does not contain chitin and it is therefore reasonable to speculate that Bgs proteins and (1,3)β-D-glucans have specialized to assume multiple essential functions. In this sense, Bgs1p would mimic budding yeast Chs2p, responsible for the synthesis of the primary septum (Schmidt et al., 2002), while Bgs4p would mimic Fks1p and Fks2p, which synthesize the (1,3)β-D-glucan of the secondary septum and cell wall, or Chs1p, which protects the cell against

an excess of cell wall degradation. However, the *S. pombe* model becomes more complicated because it contains two other proteins - Bgs3p and Ags1p/Mok1p - that are essential for cell wall construction. The specific role of each of these proteins is not yet known, although it is reasonable to assume that they have specific and separate functions during cell wall synthesis, as is the case for the three chitin synthases in *S. cerevisiae* (Shaw et al., 1991).

The requirements of Bgs4p localization during septation are only partially coincident with those of Bgs1p. Both depend on the contractile ring, but only Bgs1p fully depends on the SIN. Bgs4p does not depend on SIN proteins to internalize from the tips during mitosis. Furthermore, it depends only indirectly on the SIN to localize to the medial ring, and only when no septum has been initiated. When some septum material is present, as in the *cdc14-118* mutant, Bgs4p is able to localize to the contractile ring in the absence of a functional SIN. Nonetheless, Bgs4p localization is not sufficient to continue septum synthesis and it eventually resumes its localization to the poles. This suggests that a pre-made septum material, probably (1,3)β-D-glucan from the primary septum, acts as a landmark for Bgs4p localization, and that Bgs1p - and hence the SIN - would be needed only for Bgs4p to continue septum synthesis.

In the ring positioning mutant *mid1-366*, it was observed that CW-stained septum material overlapped Bgs1p localization but not necessarily that of Bgs4p. This result, and the fact that in a normal septum CW staining appears before the arrival of Bgs4p, indicates that at least part of the CW-stained septum material is not made by Bgs4p. Furthermore, considering that GFP-Bgs4p is functional in the *mid1* mutant, as it is in the wild-type *GFP-bgs4*$^{+}$ *bgs4*Δ strain, the product made by Bgs4p would not be stained by CW (compare arrowhead and arrow positions in *mid1* mutant in Figure 5). This suggests that CW could discriminate two different (1,3)β-D-glucan products probably comprising two Bgs proteins, which is consistent with the idea that CW recognizes fibrillar structures such as linear (1,3)β-D-glucan, proposed to be synthesized by Bgs1p.

We analyzed the role of F-actin in Bgs4p localization and observed that F-actin function is necessary for Bgs4p delocalization and relocalization but not for its stable maintenance at the growing zones. Some of these requirements have also been reported for other Bgs/Fks homologues. F-actin is

necessary for the localization, but not the maintenance, of Bgs1p at the cell division ring; it is not required for Bgs3p maintenance at the growing sites, and it is needed for Fks1p depolarization and repolarization (Delley and Hall, 1999; Liu et al., 2002; Martin et al., 2003). It is reasonable to assume that all Bgs/Fks family members share the same F-actin requirements, needed for their transport to or their internalization from the plasma membrane but dispensable for their maintenance at the growing sites as part of the plasma membrane.

Bgs2p is essential for sporulation (Liu et al., 2000; Martin et al., 2000), but this does not imply that all the (1,3)β-D-glucan of the spore wall is due to Bgs2p. In fact, Bgs1p (Cortes et al., 2002) and Bgs4p display a specific but different localization pattern during spore formation, suggesting a specific role for Bgs1p and Bgs4p in spore wall synthesis. Although not confirmed, it is very likely that Bgs3p would also be present during spore maturation. In fact, gene expression analysis using DNA microarrays has shown that the four *bgs* genes are induced during the sporulation program (Mata et al., 2002). Although *bgs2*$^+$ presents the highest induction of expression, *bgs1*$^+$, *bgs3*$^+$ and *bgs4*$^+$ exhibit an induction similar to that of the essential sporulation-specific chitin synthase gene *chs1*$^+$ (Arellano et al., 2000). Further study will be necessary to ascertain the specific role of each *bgs* in spore wall formation. We found that during the mating progression Bgs4p appeared localized first in P ($h^+$) cells and later in M ($h^-$) cells. This asymmetry suggests that Bgs4p localization forms part of the sequential pheromone response process between mating partners. At first, only M cells produce a pheromone (M factor), which induces P cells to form a mating projection and to produce P factor. Then, the P factor induces M cells to form the mating projections (Nielsen and Davey, 1995).

*S. pombe* is the only known model system containing four essential Bgs proteins that are presumed to synthesize similar (1,3)β-D-glucans. Bgs2p is specific for sporulation while Bgs1p and Bgs3p do not have a clear function. Bgs4p is the only subunit found to be necessary for cell integrity. Our Bgs4p results point to its involvement 1) in the synthesis of an essential cell wall and septum (1,3)β-D-glucan, and 2) in a crucial repair mechanism against excess cell wall degradation during cell division. In sum, this is an appealing system but further experimental work will be needed to ascertain the functions of the other subunits, Bgs1p and Bgs3p, as possible GS catalytic subunits, as well as to

determine their specific role in the fission yeast life cycle.

## ACKNOWLEDGMENTS

We wish to thank P. Pérez and B. Santos for a critical reading of the manuscript, and N. Skinner for language revision. We thank P. Munz, R. Egel, M. Yanagida, P. Nurse and F. Chang for the generous gift of strains and R. Y. Tsien for kindly providing *mRFP*-containing plasmid. J. C. G. C. and E. C. acknowledge support from a fellowship granted by Consejo Superior de Investigaciones Científicas and Ministerio de Educación y Ciencia (Spain), respectively. This work was supported by grants BIO2000-1448 and BIO2003-01040 from the Comisión Interministerial de Ciencia y Tecnología, and CSI04/03 from the Junta de Castilla y León, Spain.

## REFERENCES

**Alfa, C., Fantes, P., Hyams, J., McLeod, M. and Warbrick, E.** (1993). Experiments with fission yeast: a laboratory course manual. Cold Spring Harbor, N.Y.: Cold Spring Harbor Laboratory Press.

**Arellano, M., Cartagena-Lirola, H., Nasser Hajibagheri, M. A., Durán, A. and Valdivieso, M. H.** (2000). Proper ascospore maturation requires the *chs1*$^{+}$ chitin synthase gene in *Schizosaccharomyces pombe*. *Mol Microbiol* **35**, 79-89.

**Arellano, M., Coll, P. M. and Pérez, P.** (1999a). Rho GTPases in the control of cell morphology, cell polarity, and actin localization in fission yeast. *Microsc Res Tech* **47**, 51-60.

**Arellano, M., Durán, A. and Pérez, P.** (1996). Rho1 GTPase activates the (1-3)β-D-glucan synthase and is involved in *Schizosaccharomyces pombe* morphogenesis. *Embo J* **15**, 4584-4591.

**Arellano, M., Valdivieso, M. H., Calonge, T. M., Coll, P. M., Durán, A. and Pérez, P.** (1999b). *Schizosaccharomyces pombe* protein kinase C homologues, pck1p and pck2p, are targets of rho1p and rho2p and differentially regulate cell integrity. *J. Cell Sci.* **112**, 3569-3578.

**Bahler, J., Steever, A. B., Wheatley, S., Wang, Y., Pringle, J. R., Gould, K. L. and McCollum, D.** (1998). Role of polo kinase and Mid1p in determining the site of cell division in fission yeast. *J Cell Biol* **143**, 1603-1616.

**Balasubramanian, M. K., Bi, E. and Glotzer, M.** (2004). Comparative analysis of cytokinesis in budding yeast, fission yeast and animal cells. *Curr Biol* **14**, R806-818.

**Balasubramanian, M. K., Hirani, B. R., Burke, J. D. and Gould, K. L.** (1994). The *Schizosaccharomyces pombe cdc3*$^{+}$ gene encodes a profilin essential for cytokinesis. *J Cell Biol* **125**, 1289-1301.

**Browning, H., Hackney, D. D. and Nurse, P.** (2003). Targeted movement of cell end factors in fission yeast. *Nat Cell Biol* **5**, 812-818.

**Brunner, D. and Nurse, P.** (2000). New concepts in fission yeast morphogenesis. *Philos Trans R Soc Lond B Biol Sci* **355**, 873-877.

**Cabib, E., Roh, D. H., Schmidt, M., Crotti, L. B. and Varma, A.** (2001). The yeast cell wall and septum as paradigms of cell growth and morphogenesis. *J Biol Chem* **276**, 19679-19682.

**Campbell, R. E., Tour, O., Palmer, A. E., Steinbach, P. A., Baird, G. S., Zacharias, D. A. and Tsien, R. Y.** (2002). A monomeric red fluorescent protein. *Proc Natl Acad Sci U S A* **99**, 7877-7882.

**Castro, C., Ribas, J. C., Valdivieso, M. H., Varona, R., del Rey, F. and Durán, A.** (1995). Papulacandin B resistance in budding and fission yeasts: isolation and characterization of a gene involved in (1,3)β-D-glucan synthesis in *Saccharomyces cerevisiae*. *J Bacteriol* **177**, 5732-5739.

**Cerutti, L. and Simanis, V.** (1999). Asymmetry of the spindle pole bodies and spg1p GAP segregation during mitosis in fission yeast. *J Cell Sci* **112**, 2313-2321.

**Chang, F. and Peter, M.** (2003). Yeasts make their mark. *Nat Cell Biol* **5**, 294-299.

**Chang, F., Woollard, A. and Nurse, P.** (1996). Isolation and characterization of fission yeast mutants defective in the assembly and placement of the contractile actin ring. *J Cell Sci* **109**, 131-142.

**Cortes, J. C., Ishiguro, J., Duran, A. and Ribas, J. C.** (2002). Localization of the (1,3)β-D-glucan synthase catalytic subunit homologue Bgs1p/Cps1p from fission yeast suggests that it is

involved in septation, polarized growth, mating, spore wall formation and spore germination. *J Cell Sci* **115**, 4081-4096.

**Delley, P. A. and Hall, M. N.** (1999). Cell wall stress depolarizes cell growth via hyperactivation of *RHO1*. *J Cell Biol* **147**, 163-174.

**Dijkgraaf, G. J., Abe, M., Ohya, Y. and Bussey, H.** (2002). Mutations in Fks1p affect the cell wall content of β-1,3- and β-1,6-glucan in *Saccharomyces cerevisiae*. *Yeast* **19**, 671-690.

**Douglas, C. M., Foor, F., Marrinan, J. A., Morin, N., Nielsen, J. B., Dahl, A. M., Mazur, P., Baginsky, W., Li, W., El-Sherbeini, M. et al.** (1994). The *Saccharomyces cerevisiae FKS1 (ETG1)* gene encodes an integral membrane protein which is a subunit of 1,3-β-D-glucan synthase. *Proc. Natl. Acad. Sci. USA* **91**, 12907-12911.

**Drgonova, J., Drgon, T., Roh, D. H. and Cabib, E.** (1999). The GTP-binding protein Rho1p is required for cell cycle progression and polarization of the yeast cell. *J Cell Biol* **146**, 373-387.

**Drgonova, J., Drgon, T., Tanaka, K., Kollar, R., Chen, G.-C., Ford, R. A., Chan, C. S. M., Takai, Y. and Cabib, E.** (1996). Rho1p, a yeast protein at the interface between cell polarization and morphogenesis. *Science* **272**, 277-279.

**Duran, A. and Perez, P.** (2004). Cell wall synthesis. In *Molecular biology of Schizosaccharomyces pombe. Genetics, genomics and beyond*, (ed. R. Egel), pp. 269-279. Berlin: Springer Verlag.

**Egel, R.** (1984). Two tightly linked silent cassettes in the mating-type region of *Schizosaccharomyces pombe*. *Curr. Genet.* **8**, 199-203.

**Eng, W.-K., Faucette, L., McLaughlin, M. M., Cafferkey, R., Koltin, Y., Morris, R. A., Young, P. R., Johnson, R. K. and Livi, G. P.** (1994). The yeast *FKS1* gene encodes a novel membrane protein, mutations in which confer FK506 and cyclosporin A hypersensitivity and calcineurin-dependent growth. *Gene* **151**, 61-71.

**Fankhauser, C., Reymond, A., Cerutti, L., Utzig, S., Hofmann, K. and Simanis, V.** (1995). The *S. pombe cdc15* gene is a key element in the reorganization of F-actin at mitosis. *Cell* **82**, 435-444.

**Fernandez-Abalos, J. M., Fox, H., Pitt, C., Wells, B. and Doonan, J. H.** (1998). Plant-adapted green fluorescent protein is a versatile vital reporter for gene expression, protein localization and mitosis in the filamentous fungus, *Aspergillus nidulans*. *Mol Microbiol* **27**, 121-130.

**Furge, K. A., Wong, K., Armstrong, J., Balasubramanian, M. and Albright, C. F.** (1998). Byr4 and Cdc16 form a two-component GTPase-activating protein for the Spg1 GTPase that controls septation in fission yeast. *Curr Biol* **8**, 947-954.

**Garrett-Engele, P., Moilanen, B. and Cyert, M. S.** (1995). Calcineurin, the $Ca^{2+}$/calmodulin-dependent protein phosphatase, is essential in yeast mutants with cell integrity defects and in mutants that lack a functional vacuolar $H^{+}$-ATPase. *Mol. Cell. Biol.* **15**, 4103-4114.

**Gietz, R. D., Schiestl, R. H., Willems, A. R. and Woods, R. A.** (1995). Studies on the transformation of intact yeast cells by the LiAc/SS- DNA/PEG procedure. *Yeast* **11**, 355-360.

**Guertin, D. A., Chang, L., Irshad, F., Gould, K. L. and McCollum, D.** (2000). The role of the sid1p kinase and cdc14p in regulating the onset of cytokinesis in fission yeast. *Embo J* **19**, 1803-1815.

**Guertin, D. A., Trautmann, S. and McCollum, D.** (2002). Cytokinesis in eukaryotes. *Microbiol Mol Biol Rev* **66**, 155-178.

**Hayles, J. and Nurse, P.** (2001). A journey into space. *Nat Rev Mol Cell Biol* **2**, 647-656.

**Humbel, B. M., Konomi, M., Takagi, T., Kamasawa, N., Ishijima, S. A. and Osumi, M.** (2001). In situ localization of β-glucans in the cell wall of *Schizosaccharomyces pombe*. *Yeast* **18**, 433-444.

**Inoue, S. B., Takewaki, N., Takasuka, T., Mio, T., Adachi, M., Fujii, Y., Miyamoto, C., Arisawa, M., Furuichi, Y. and Watanabe, T.** (1995). Characterization and gene cloning of 1,3-β-D-glucan synthase from *Saccharomyces cerevisiae*. *Eur J Biochem* **231**, 845-854.

**Ishiguro, J. and Kobayashi, W.** (1996). An actin point-mutation neighboring the 'hydrofobic plug' causes defects in the maintenance of cell polarity and septum organization in the fission yeast *Schizosaccharomyces pombe*. *FEBS Lett.* **392**, 237-241.

**Ishiguro, J., Saitou, A., Duran, A. and Ribas, J. C.** (1997). *cps1*$^{+}$, a *Schizosaccharomyces pombe* gene homolog of *Saccharomyces cerevisiae FKS* genes whose mutation confers hypersensitivity to cyclosporin A and papulacandin B. *J. Bacteriol.* **179**, 7653-7662.

**Kang, M. S. and Cabib, E.** (1986). Regulation of fungal cell wall growth: a guanine nucleotide-binding proteinaceous component required for activity of (1,3)-β-D-glucan synthase. *Proc. Natl. Acad. Sci. USA* **83**, 5808-5812.

**Katayama, S., Hirata, D., Arellano, M., Pérez, P. and Toda, T.** (1999). Fission yeast α-glucan synthase Mok1 requires the actin cytoskeleton to localize the sites of growth and plays an essential role in cell morphogenesis downstream of protein kinase C function. *J Cell Biol* **144**, 1173-1186.

**Kobori, H., Yamada, N., Taki, A. and Osumi, M.** (1989). Actin is associated with the formation of the cell wall in reverting protoplasts of the fission yeast *Schizosaccharomyces pombe*. *J Cell Sci* **94**, 635-646.

**Krapp, A., Gulli, M. P. and Simanis, V.** (2004). SIN and the Art of Splitting the Fission Yeast Cell. *Curr Biol* **14**, R722-730.

**Krapp, A., Schmidt, S., Cano, E. and Simanis, V.** (2001). *S. pombe* cdc11p, together with sid4p, provides an anchor for septation initiation network proteins on the spindle pole body. *Curr Biol* **11**, 1559-1568.

**Le Goff, X., Woollard, A. and Simanis, V.** (1999). Analysis of the *cps1* gene provides evidence for a septation checkpoint in *Schizosaccharomyces pombe. Mol. Gen. Genet.* **262**, 163-172.

**Liu, J., Tang, X., Wang, H. and Balasubramanian, M.** (2000). Bgs2p, a 1,3-β-glucan synthase subunit, is essential for maturation of ascospore wall in *Schizosaccharomyces pombe*. *FEBS Lett* **478**, 105-108.

**Liu, J., Tang, X., Wang, H., Oliferenko, S. and Balasubramanian, M. K.** (2002). The Localization of the Integral Membrane Protein Cps1p to the Cell Division Site is Dependent on the Actomyosin Ring and the Septation-Inducing Network in *Schizosaccharomyces pombe*. *Mol Biol Cell* **13**, 989-1000.

**Liu, J., Wang, H., McCollum, D. and Balasubramanian, M. K.** (1999). Drc1p/Cps1p, a 1,3-β-glucan synthase subunit, is essential for division septum assembly in *Schizosaccharomyces pombe*. *Genetics* **153**, 1193-1203.

**Marks, J., Hagan, I. M. and Hyams, J. S.** (1986). Growth polarity and cytokinesis in fission yeast: the role of the cytoskeleton. *J Cell Sci Suppl* **5**, 229-241.

**Martin, V., Garcia, B., Carnero, E., Duran, A. and Sanchez, Y.** (2003). Bgs3p, a putative 1,3-β-glucan synthase subunit, is required for cell wall assembly in *Schizosaccharomyces pombe*. *Eukaryot Cell* **2**, 159-169.

**Martin, V., Ribas, J. C., Carnero, E., Duran, A. and Sanchez, Y.** (2000). *bgs2*$^{+}$, a sporulation-specific glucan synthase homologue is required for proper ascospore wall maturation in fission yeast. *Mol Microbiol* **38**, 308-321.

**Martin-Cuadrado, A. B., Duenas, E., Sipiczki, M., Vazquez de Aldana, C. R. and del Rey, F.** (2003). The endo-β-1,3-glucanase eng1p is required for dissolution of the primary septum during cell separation in *Schizosaccharomyces pombe*. *J Cell Sci* **116**, 1689-1698.

**Mata, J., Lyne, R., Burns, G. and Bahler, J.** (2002). The transcriptional program of meiosis and sporulation in fission yeast. *Nat Genet* **32**, 143-147.

**Mazur, P., Morin, N., Baginsky, W., El-Sherbeini, M., Clemas, J. A., Nielsen, J. B. and Foor, F.** (1995). Differential expression and function of two homologous subunits of yeast 1,3-β-D-glucan synthase. *Mol Cell Biol* **15**, 5671-5681.

**Moreno, M. B., Duran, A. and Ribas, J. C.** (2000). A family of multifunctional thiamine-repressible expression vectors for fission yeast. *Yeast* **16**, 861-872.

**Moreno, S., Klar, A. and Nurse, P.** (1991). Molecular genetic analysis of fission yeast *Schizosaccharomyces pombe*. *Meth. Enzymol.* **194**, 795-823.

**Nielsen, O. and Davey, J.** (1995). Pheromone communication in the fission yeast *Schizosaccharomyces pombe*. *Semin Cell Biol* **6**, 95-104.

**Nurse, P., Thuriaux, P. and Nasmyth, K.** (1976). Genetic control of the cell division cycle in the fission yeast *Schizosaccharomyces pombe*. *Mol Gen Genet* **146**, 167-178.

**Pelham, R. J. and Chang, F.** (2002). Actin dynamics in the contractile ring during cytokinesis in fission yeast. *Nature* **419**, 82-86.

**Pelham, R. J., Jr. and Chang, F.** (2001). Role of actin polymerization and actin cables in actin-patch movement in *Schizosaccharomyces pombe*. *Nat Cell Biol* **3**, 235-244.

**Perez, P. and Ribas, J. C.** (2004). Cell wall analysis. *Methods* **33**, 245-251.

**Ram, A. F. J., Brekelmans, S. S. C., Oehlen, L. J. W. M. and Klis, F. M.** (1995). Identification of two cell cycle regulated genes affecting the β1,3-glucan content of cell walls in *Saccharomyces cerevisiae*. *FEBS Lett.* **358**, 165-170.

**Ribas, J. C., Díaz, M., Durán, A. and Pérez, P.** (1991). Isolation and characterization of *Schizosaccharomyces pombe* mutants defective in cell wall (1-3)β-D-glucan. *J Bacteriol* **173**, 3456-3462.

**Roncero, C.** (2002). The genetic complexity of chitin synthesis in fungi. *Curr Genet* **41**, 367-378.

**Sambrook, J. and Russell, D. W.** (2001). Molecular cloning: A laboratory manual. Cold Spring Harbor, N.Y.: Cold Spring Harbor Laboratory Press.

**Sawin, K. E. and Snaith, H. A.** (2004). Role of microtubules and tea1p in establishment and maintenance of fission yeast cell polarity. *J Cell Sci* **117**, 689-700.

**Schmidt, M., Bowers, B., Varma, A., Roh, D. H. and Cabib, E.** (2002). In budding yeast, contraction of the actomyosin ring and formation of the primary septum at cytokinesis depend on each other. *J Cell Sci* **115**, 293-302.

**Shaw, J. A., Mol, P. C., Bowers, B., Silverman, S. J., Valdivieso, M. H., Duran, A. and Cabib, E.** (1991). The function of chitin synthases 2 and 3 in the *Saccharomyces cerevisiae* cell cycle. *J Cell Biol* **114**, 111-123.

**Sohrmann, M., Fankhauser, C., Brodbeck, C. and Simanis, V.** (1996). The *dmf1/mid1* gene is essential for correct positioning of the division septum in fission yeast. *Genes Dev* **10**, 2707-2719.

**Utsugi, T., Minemura, M., Hirata, A., Abe, M., Watanabe, D. and Ohya, Y.** (2002). Movement of yeast 1,3-β-glucan synthase is essential for uniform cell wall synthesis. *Genes Cells* **7**, 1-9.

**Verde, F., Mata, J. and Nurse, P.** (1995). Fission yeast cell morphogenesis: Identification of new genes and analysis of their role during the cell cycle. *J. Cell Biol.* **131**, 1529-1538.

**FIGURE LEGENDS**

Figure 1. *bgs4*$^+$ *cwg1*$^+$and *orb11*$^+$ are the same gene.

**(A)** *bgs4*$^+$ suppresses the lethal thermosensitive phenotype of *cwg1-1* mutant cells. Wild-type (*leu1-32* h$^-$) and *cwg1-1* (*cwg1-1 leu1-32* h$^-$) cells transformed with the empty plasmid pAL-KS$^+$ or the plasmid pAL-*bgs4*$^+$ (pJG1) and grown at 28°C were streaked out on EMM plates and incubated at 37°C for 4 days. **(B)** *bgs4*$^+$ suppresses the in vitro GS defect of cell extracts from *cwg1-1* cells grown at 37°C. The same cells as in (A) were grown on EMM + 1.2M sorbitol liquid medium at 37°C and the GS activity of cell extracts was analyzed at 30°C, as described in Methods. Values in parentheses are the specific activity average, calculated from three independent extracts. **(C)** Both homozygous *cwg1-1* / *cwg1-1* and heterozygous *cwg1-1* / *bgs4*Δ diploids present the same thermosensitive spherical morphology. Phase-contrast and Calcofluor white (CW) UV staining micrographs of log-phase cells grown on EMM liquid medium at 37°C for 12 hours. **(D)** *bgs4*$^+$ suppresses the thermosensitive morphology of *orb11-59* cells. Wild-type and *orb11-59* cells transformed with the indicated plasmids were grown at 37°C for 24 hours and visualized as in (C). Bars, 10 μm.

Figure 2. Absence of *bgs4*$^+$ promotes lysis in both germinating spores and growing cells.

**(A)** *bgs4*Δ spores are able to germinate but lyse before their first cell division. Tetrads from *bgs4*$^+$/*bgs4*Δ strain were dissected on YES and YES + 1.2M sorbitol medium and incubated at 28°C for 1 and 2 days, respectively. Photographs of a tetrad representative for each case, with two *bgs4*$^+$ colonies and two germinated *bgs4*Δ spores lysing before cell division, are shown. Arrows indicate the germination site, with cell projections swelling up (+Sorbitol) and finally lysing (-Sorbitol). **(B)** *bgs4*$^+$ shut-off promotes cell growth arrest after 14 hours of growth on EMM + thiamine medium. Sorbitol only partially protects the *bgs4*Δ cells and delays the arrest of cell growth to 17 hours. Log-phase control and *bgs4*Δ p81x-*bgs4*$^+$ cells were grown on EMM or EMM + 1.2M sorbitol liquid media at 32°C, either in the absence (-T, induced) or in the presence (+T, repressed) of thiamine. Cell growth was monitored after 12 or 15 hours of growth with thiamine, depending on the absence or the presence

of sorbitol in the medium, respectively. **(C)** *bgs4*$^+$ shut-off promotes cell lysis and release of cytoplasmic material from either the growing pole or the septum region. Log-phase *bgs4*Δ p81x-*bgs4*$^+$ cells grown on EMM + T liquid medium at 32°C for 18 hours were visualized as in Fig. 1C. **(D)** *bgs4*$^+$ shut-off induces a dramatic decrease in GS activity. Log-phase *bgs4*Δ p81x-*bgs4*$^+$ cells grown on EMM ± T as in (B) were collected at the indicated times and assayed for GS activity as in Fig. 1B. **(E)** *bgs4*$^+$ shut-off produces actin delocalization and depolymerization prior to cell lysis. *bgs4*Δ p81x-*bgs4*$^+$ cells grown on EMM + T as in (C) were collected at the indicated times, fixed, and stained with rodamine-conjugated phalloidin. Bars, 5 μm.

Figure 3. *bgs4*$^+$overexpression produces defects in cell integrity.

**(A)** *bgs4*$^+$ overexpression causes cell growth arrest, which is delayed in the presence of sorbitol. Log-phase wild-type and *bgs4*Δ p3x-*bgs4*$^+$ cells were grown and monitored after 18 hours of growth in the absence of thiamine as in Fig. 2B. **(B)** Rounded and elongated morphology of *bgs4*$^+$-overexpressing cells. Log-phase *bgs4*Δ p3x-*bgs4*$^+$ cells were grown on EMM liquid medium at 32°C and visualized at the indicated times as in Fig. 1C. **(C)** *bgs4*$^+$ overexpression induces actin delocalization in rounded cells. *bgs4*Δ p3x-*bgs4*$^+$ cells grown on EMM liquid medium at 32°C for 24 hours were stained for actin visualization as in Fig. 2E. **(D)** *bgs4*$^+$ overexpression produces a gradual reduction in GS activity. Log-phase *bgs4*Δ p3x-*bgs4*$^+$ cells grown on EMM as in (A) were collected at the indicated times and assayed for GS activity as in Fig. 1B. Bars, 10 μm.

Figure 4. Bgs4p localizes to the growing regions: one or both poles, medial ring and septum.

**(A)** CW staining and GFP-Bgs4p localization along the mitotic cell cycle. Early-logarithmic phase cells (*GFP-bgs4*$^+$ *bgs4*Δ), grown on YES liquid medium at 28°C, were visualized for CW staining and GFP fluorescence. CW was added at 50 μg/ml followed by immediate examination of the cells. A total of 436 cells from 41 different images were ordered and analyzed. Cells representative of each cell cycle step were selected and ordered to show a cell cycle progression. Bar, 2 μm. **(B)** Magnification of CW staining and GFP-Bgs4p localization to the medial ring and along the plasma membrane during

septum formation. Bar, 1 μm. **(C)** Bgs4p localizes to the medial ring later than Bgs1p. CW staining and GFP-Bgs1p or GFP-Bgs4p localization during mitosis and cytokinesis. *GFP-bgs1*$^{+}$ *bgs1*Δ and *GFP-bgs4*$^{+}$ *bgs4*Δ cells were grown as in (A), ethanol-fixed, and analyzed for GFP and CW / Hoechst staining. A total of 132 GFP-Bgs1p- and 76 GFP-Bgs4p-expressing mitotic cells, from 35 and 16 different images respectively, were ordered and analyzed. Cells representative of the anaphase to the cytokinesis process were selected and ordered to show a progression. Bar, 2 μm.

Figure 5. Bgs4p localization during septation depends on medial ring formation and positioning, but the SIN proteins may be dispensable for its localization to the medial ring and septum.

*GFP-bgs4*$^{+}$ *bgs4*Δ mutant cells were grown as in Fig. 4A, shifted to 32°C (*cdc3-6*, *cdc15-140* and *cdc16-116*) for 4 hours or to 37°C (*mid1-366*, *cdc14-118*) for 3 to 6 hours, and visualized as in Fig. 4A, except *cdc14-118* cells, which were also analyzed for nucleus staining as in Fig. 4C. Cells representative of the different mutant phenotypes are shown. In *mid1-366*, cells with overlapping and non-overlapping CW (arrowhead) and GFP-Bgs4p (arrow) fluorescence are shown. In *cdc14-118*, cells representative of the phenotype at different times are shown, including cells displaying a partial septum (arrowhead) synthesized before they expressed the mutant phenotype, some of them with GFP-Bgs4p (arrow) localized to the partial septum structure. Bars, 2 μm.

Figure 6. Bgs4p localization depends on polarity establishment proteins and on the actin cytoskeleton.

**(A)** Bgs4p localizes to the altered growing poles and septa in the end-marker mutants *tea1-1*, *tea2-1* and *tea2-1 cdc11-119*. **(B)** Bgs4p localizes all around the cell membrane and septum in the actin mutant *cps8-188*. *GFP-bgs4*$^{+}$ *bgs4*Δ mutant cells were grown as in Fig. 4A, shifted to 37°C for 6 hours (*cps8-188*, *tea2-1 cdc11-119*) or 8 hours (*tea1-1* and *tea2-1*), and visualized as in Fig. 4A. Bars, 2 μm.

Figure 7. Polarized F-actin is necessary for Bgs4p delocalization from and relocalization to the growing regions, poles and septum, but not for its stable maintenance at the growing zones.

**(A)** Maintenance of Bgs4p to the medial ring and poles does not require the F-actin function. Early-logarithmic phase cells (*RFP-bgs4*$^{+}$ *bgs4*Δ *crn1*$^{+}$*-GFP*) grown on YES liquid medium at 28°C were transferred to YES medium containing Lat A (100 μM) or an equal volume of DMSO as control and incubated at 28°C for 15 minutes. Cells grown in the presence of DMSO displayed the same RFP-Bgs4p and Crn1p-GFP localization as initial control cells (data not shown). The Lat A-treated cells were washed, transferred to fresh YES medium, and incubated at 28°C for 3 hours. Cells were collected at the indicated times, fixed, and analyzed for RFP (Bgs4p) and GFP (actin-associated Crn1p) fluorescence. **(B)** The F-actin cytoskeleton is needed for Bgs4p relocalization to the growing regions. Cells grown as in (A) were exposed to stress conditions (high temperature and the absence of nitrogen) for 2 hours to induce Bgs4p and F-actin patches delocalization. Then, the cells were transferred to YES medium and incubated at 28°C for 2 hours in the presence of Lat A or DMSO (-Lat A control). Cells were collected at the indicated times and analyzed as in (A). **(C)** The F-actin cytoskeleton is necessary for Bgs4p delocalization from the growing zones upon stress treatment. Cells were grown and treated with Lat A as in (A) to induce actin depolymerization and to maintain Bgs4p polarized. Then, the cells were washed and exposed to stress conditions (absence of nitrogen) in the presence of Lat A or DMSO (-Lat A control). Cells were collected at the indicated times and analyzed as in (A).

Figure 8. Bgs4p is present and localized to all sites of cell wall synthesis during sexual differentiation. Homothallic *GFP-bgs4*$^{+}$ *bgs4*Δ h$^{90}$ cells grown on EMM at 28°C up to the early-stationary phase were transferred onto SPA plates and incubated at 28°C. Samples were collected at 3, 5, 8, 24 and 48 hours, resuspended in CW-containing (50 μg/ml) EMM medium, and visualized as in Fig. 4A. A total of 435 mating cells and zygotes from 86 different images were ordered and analyzed. Cells and zygotes representative of each mating and sporulation step were selected and ordered to show a sexual phase progression. Bar, 2 μm.

Figure 9. Bgs4p localizes to the mating projections in an ordered mating type-dependent sequence,

appearing first in P ($h^+$) cells and later in M ($h^-$) cells.

Early-logarithmic phase cells (*GFP-bgs4*$^+$ *bgs4*Δ $h^-$ and $h^+$, and *RFP-bgs4*$^+$ *bgs4*Δ $h^-$ and $h^+$) grown on EMM at 28°C were collected, washed, and mixed in equal cell amounts ($h^+$ *GFP-bgs4*$^+$ x $h^-$ *RFP-bgs4*$^+$, and $h^+$ *RFP-bgs4*$^+$ x $h^-$ *GFP-bgs4*$^+$). Cell mixtures were transferred onto SPA plates and incubated at 28°C. Samples were collected at 30-minutes intervals from 0 to 5 hours, ethanol-fixed, and examined for GFP and RFP fluorescence. Merged images with GFP (green) and RFP (red) fluorescence are shown. Arrowheads show the first time point at which $h^+$ cells develop mating projections and localize Bgs4p (GFP or RFP). Arrows show the first time point at which mating projections and localized Bgs4p (GFP or RFP) are detected in $h^-$ cells.

Figure 10. Bgs4p localizes to the different sites of cell wall growth during spore germination.

The homothallic *GFP-bgs4*$^+$ *bgs4*Δ $h^{90}$ strain was grown and sporulated for 7 days as in Fig. 8. The spores were collected and incubated in YES liquid medium at 28°C. Samples were taken at 3, 7, 9 and 11 hours, and examined as in Fig. 4A. A total of 252 spores from 42 different images were ordered and analyzed. Spores illustrative of each germination step were selected and ordered to show a germination progression. Bar, 2 μm.

**TABLE 1. Fission yeast strains used in this study.**

| Strain | Genotype | Source |
|---|---|---|
| 33 | 972 $h^-$ | P. Munz[a] |
| 38 | 968 $h^{90}$ | P. Munz[a] |
| 77 | *leu1-32* $h^-$ | J. C. Ribas |
| 328 | *leu1-32 bgs4*$^+$*::bgs4*$^+$*:leu1*$^+$ $h^-$ | This study |
| 27 | *lys1-131* mat2P-B102 | R. Egel[b] |
| 284 | *leu1-32 ura4-Δ18 his3-Δ1* $h^-$ | J. C. Ribas |
| 285 | *leu1-32 ura4-Δ18 his3-Δ1* $h^+$ | J. C. Ribas |
| 470 | *leu1-32 ura4-Δ18 his3-Δ1* $h^{90}$ | J. C. Ribas |
| 315 | *leu1-32/leu1-32 ura4-Δ18/ura4-Δ18 ade6-M210/ade6-M216* $h^-/h^+$ | This study |
| 303 | *cwg1-1 ura4-Δ18 ade5-36* $h^+$ | This study |
| 304 | *ppe1::ura4*$^+$ *leu1-32 ura4-Δ18* $h^-$ pPH101 | M. Yanagida[c] |
| 132 | *cwg1-1 leu1-32* $h^-$ | J. C. Ribas |
| 133 | *cwg1-1 leu1-32* $h^+$ | J. C. Ribas |
| 86 | *cwg1-1 lys1-131* mat2P-B102 | J. C. Ribas |
| 803 | *cwg1-1 leu1-32* $P_{bgs4}^+$*::bgs4*$^+$*:leu1*$^+$ $h^-$ | This study |
| 156 | *cwg1-2 leu1-32* $h^-$ | J. C. Ribas |
| 805 | *cwg1-2 leu1-32* $P_{bgs4}^+$*::bgs4*$^+$*:leu1*$^+$ $h^-$ | This study |
| 544 | *orb11-59 leu1-32 ade6-M210* $h^-$ | P. Nurse[d] |
| 796 | *orb11-59 leu1-32 ade6-M210* $P_{bgs4}^+$*::bgs4*$^+$*:leu1*$^+$ $h^-$ | This study |
| 635 | *mid1-366 leu1-32* $h^+$ | P. Nurse[d] |
| 439 | *cdc3-6 leu1-32* $h^+$ | This study |
| 572 | *cdc14-118 leu1-32* $h^+$ | This study |
| 574 | *cdc15-140 leu1-32* $h^+$ | This study |
| 581 | *cdc16-116 ura4-Δ18* $h^-$ | J. C. Ribas |
| 583 | *tea1-1 leu1-32* $h^-$ | P. Nurse[d] |
| 585 | *tea2-1 cdc11-119 leu1-32* $h^-$ | P. Nurse[d] |
| 254 | *cps8-188 leu1-32* $h^+$ | This study |
| 962 | *leu1-32 ura4-Δ18 ade6 crn1*$^+$*-GFP:KanMX6* $h^+$ | F. Chang[e] |
| 341 | *leu1-32/leu1-32 ura4-Δ18/ura4-Δ18 ade6-M210/ade6-M216 bgs4*$^+$*/bgs4Δ::ura4*$^+$ $h^-/h^+$ | This study |
| 404 | *leu1-32 ura4-Δ18 ade6-M216 bgs4Δ::ura4*$^+$ $h^-$ pJG1 (pAL-*bgs4*$^+$) | This study |
| 425 | *leu1-32 ura4-Δ18 his3-Δ1 bgs4Δ::ura4*$^+$ $h^-$ pJG1 (pAL-*bgs4*$^+$) | This study |
| 421 | *leu1-32 ura4-Δ18 his3-Δ1 bgs4Δ::ura4*$^+$ $h^-$ pJG17 (p3X-*bgs4*$^+$) | This study |
| 451 | *leu1-32 ura4-Δ18 his3-Δ1 bgs4Δ::ura4*$^+$ $h^-$ pJG18 (p41X-*bgs4*$^+$) | This study |
| 447 | *leu1-32 ura4-Δ18 his3-Δ1 bgs4Δ::ura4*$^+$ $h^-$ pJG19 (p81X-*bgs4*$^+$) | This study |
| 498 | *leu1-32 ura4-Δ18 his3-Δ1 bgs4Δ::ura4*$^+$ $h^-$ pJG33 (p81XH-*bgs4*$^+$) | This study |
| 561 | *leu1-32 ura4-Δ18 his3-Δ1 bgs4Δ::ura4*$^+$ $P_{bgs4}^+$*::GFP-bgs4*$^+$*:leu1*$^+$ $h^-$ | This study |
| 562 | *leu1-32 ura4-Δ18 his3-Δ1 bgs4Δ::ura4*$^+$ $P_{bgs4}^+$*::GFP-bgs4*$^+$*:leu1*$^+$ $h^+$ | This study |
| 978 | *leu1-32 ura4-Δ18 his3-Δ1 bgs4Δ::ura4*$^+$ $P_{bgs4}^+$*::RFP-bgs4*$^+$*:leu1*$^+$ $h^-$ | This study |
| 979 | *leu1-32 ura4-Δ18 his3-Δ1 bgs4Δ::ura4*$^+$ $P_{bgs4}^+$*::RFP-bgs4*$^+$*:leu1*$^+$ $h^+$ | This study |
| 519 | *leu1-32 ura4-Δ18 his3-Δ1 bgs1Δ::ura4*$^+$ $P_{bgs1}^+$*::GFP-bgs1*$^+$*:leu1*$^+$ $h^-$ | J. C. Ribas |
| 675 | *mid1-366 leu1-32 ura4*? *bgs4Δ::ura4*$^+$ $P_{bgs4}^+$*::GFP-bgs4*$^+$*:leu1*$^+$ $h^-$ | This study |
| 709 | *cdc3-6 leu1-32 bgs4Δ::ura4*$^+$ $P_{bgs4}^+$*::GFP-bgs4*$^+$*:leu1*$^+$ $h^-$ | This study |
| 624 | *cdc11-119 leu1-32 ura4-Δ18 his3-Δ1 bgs4Δ::ura4*$^+$ $P_{bgs4}^+$*::GFP-bgs4*$^+$*:leu1*$^+$ $h^+$ | This study |
| 602 | *cdc14-118 leu1-32 ura4-Δ18 bgs4Δ::ura4*$^+$ $P_{bgs4}^+$*::GFP-bgs4*$^+$*:leu1*$^+$ $h^+$ | This study |
| 606 | *cdc15-140 leu1-32 ura4-Δ18 his3-Δ1 bgs4Δ::ura4*$^+$ $P_{bgs4}^+$*::GFP-bgs4*$^+$*:leu1*$^+$ $h^+$ | This study |
| 626 | *cdc16-116 leu1-32 ura4-Δ18 bgs4Δ::ura4*$^+$ $P_{bgs4}^+$*::GFP-bgs4*$^+$*:leu1*$^+$ $h^-$ | This study |
| 607 | *tea1-1 leu1-32 ura4-Δ18 his3-Δ1 bgs4Δ::ura4*$^+$ $P_{bgs4}^+$*::GFP-bgs4*$^+$*:leu1*$^+$ $h^+$ | This study |
| 609 | *tea2-1 leu1-32 ura4-Δ18 his3-Δ1 bgs4Δ::ura4*$^+$ $P_{bgs4}^+$*::GFP-bgs4*$^+$*:leu1*$^+$ $h^+$ | This study |
| 620 | *tea2-1 cdc11-119 leu1-32 ura4-Δ18 bgs4Δ::ura4*$^+$ $P_{bgs4}^+$*::GFP-bgs4*$^+$*:leu1*$^+$ $h^+$ | This study |
| 714 | *cps8-188 leu1-32 ura4-*Δ18 *bgs4Δ::ura4*$^+$ $P_{bgs4}^+$*::GFP-bgs4*$^+$*:leu1*$^+$ $h^+$ | This study |
| 995 | *leu1-32 ura4-Δ18 bgs4Δ::ura4*$^+$ $P_{bgs4}^+$*::RFP-bgs4*$^+$*:leu1*$^+$ *crn1*$^+$*-GFP:KanMX6* $h^-$ | This study |
| 586 | *leu1-32 ura4-Δ18 his3-Δ1 bgs4Δ::ura4*$^+$ $P_{bgs4}^+$*::GFP-bgs4*$^+$*:leu1*$^+$ $h^{90}$ | This study |

[a]Institute of General Microbiology, University of Bern, Switzerland.
[b]Department of Genetics, University of Copenhagen, Denmark.
[c]Department of Biophysics, Kyoto University, Japan.
[d]Laboratory of Yeast Genetics and Cell Biology, The Rockefeller University, New York, USA.
[e]Department of Microbiology, Columbia university, New York, USA.

**TABLE 2. Incorporation of radioactivity from [$^{14}$C]glucose into cell wall polysaccharides during *bgs4*$^{+}$ shut-off of *S. pombe* wild-type and mutant *bgs4*Δ p81X-*bgs4*$^{+}$ strains grown at 32°C in EMM or in EMM+1.2M sorbitol, either in the absence (induced) or in the presence (repressed) of thiamine.**

| Growth | Strain | Thiamine[a] | % Incorporation of [$^{14}$C]glucose (mean ± SD)[b] | | | |
|---|---|---|---|---|---|---|
| | | | Cell wall | α-Glucan | β-Glucan | Galactomannan |
| EMM | *bgs4*Δ p81x-*bgs4*$^{+}$ | - (on) | 33.5 ± 0.8 (100)[c] | 10.1 ± 0.7 (30.1) | 19.4 ± 0.2 (57.9) | 4.0 ± 0.3 (12.0) |
| | *bgs4*Δ p81x-*bgs4*$^{+}$ | + (off) | 43.7 ± 0.1 (100) | 19.6 ± 0.5 (44.9) | 20.0 ± 0.6 (45.9) | 4.1 ± 0.2 (9.2) |
| EMM+S | *bgs4*Δ p81x-*bgs4*$^{+}$ | - (on) | 29.5 ± 0.2 (100) | 8.2 ± 0.3 (27.9) | 17.1 ± 0.2 (57.8) | 4.2 ± 0.1 (14.3) |
| | *bgs4*Δ p81x-*bgs4*$^{+}$ | + (off) | 36.3 ± 0.1 (100) | 16.5 ± 0.1 (45.5) | 15.3 ± 0.1 (42.2) | 4.5 ± 0.1 (12.3) |

[a] Induction of p81X-*bgs4*$^{+}$ maintains the *bgs4*Δ cells with wild-type GS activity and morphology. *bgs4*$^{+}$-repressed cell cultures were grown for 16 hours in the presence of thiamine. [$^{14}$C]glucose was added 4 hours before harvesting.

[b] Percentage incorporation of [$^{14}$C]glucose = cpm incorporated per fraction x 100/total cpm incorporated. Values are the means and standard deviations (SD) calculated from three independent experiments.

[c] Values in parentheses are percentages of the corresponding polysaccharide in the cell wall composition.

**TABLE 3. Incorporation of radioactivity from [$^{14}$C]glucose into cell wall polysaccharides during *bgs4*$^{+}$ overexpression of *S. pombe* wild-type and mutant *bgs4*Δ p3X-*bgs4*$^{+}$ strains grown at 32°C in EMM, either in the presence (repressed) or in the absence (overexpressed, OE) of thiamine.**

| Time (hours) | Strain | Thiamine[a] | % Incorporation of [$^{14}$C]glucose (mean ± SD)[b] | | | |
|---|---|---|---|---|---|---|
| | | | Cell wall | α-Glucan | β-Glucan | Galactomannan |
| 15[c] | *bgs4*Δ p3X-*bgs4*$^{+}$ | + | 31.8 ± 0.7 (100) | 14.2 ± 0.2 (44.6) | 15.5 ± 0.5 (48.9) | 2.1 ± 0.1 (6.5) |
| | *bgs4*Δ p3X-*bgs4*$^{+}$ | - (OE) | 31.4 ± 0.1 (100) | 15.2 ± 0.6 (48.6) | 13.5 ± 0.5 (42.8) | 2.7 ± 0.2 (8.6) |
| 30[d] | *bgs4*Δ p3X-*bgs4*$^{+}$ | + | 32.1 ± 0.7 (100) | 13.4 ± 0.6 (41.8) | 15.7 ± 0.7 (48.9) | 3.0 ± 0.2 (9.3) |
| | *bgs4*Δ p3X-*bgs4*$^{+}$ | - (OE) | 37.4 ± 0.8 (100) | 20.7 ± 1.5 (55.4) | 14.5 ± 1.4 (38.8) | 2.2 ± 0.4 (5.8) |

[a] Repression of p3X-*bgs4*$^{+}$ maintains the *bgs4*Δ cells with wild-type GS activity and morphology.

[b] Values were calculated from three independent experiments as in Table 2.

[c] [$^{14}$C]glucose was added to the cell cultures 6 hours before harvesting.

[d] [$^{14}$C]glucose was added to the cell cultures 7 hours (control cells, +thiamine) or 21 hours (*bgs4*$^{+}$-overexpressing cells, -thiamine) before harvesting.

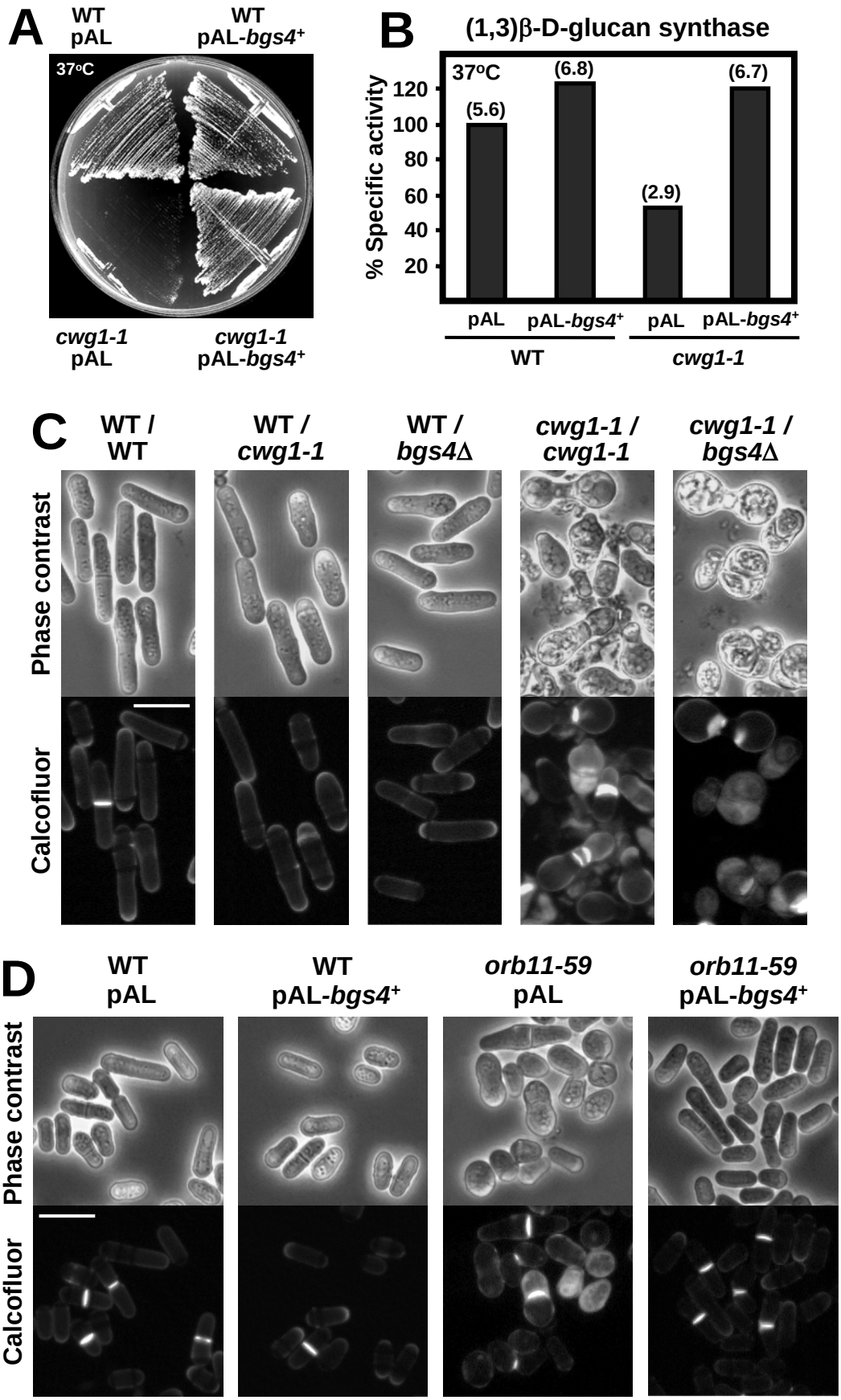
A
WT pAL
WT pAL-bgs4+
37ºC
cwg1-1 pAL
cwg1-1 pAL-bgs4+
B
(1,3)β-D-glucan synthase
% Specific activity
120
100
80
60
40
20
37ºC
(5.6)
(6.8)
(2.9)
(6.7)
pAL
pAL-bgs4+
pAL
pAL-bgs4+
WT
cwg1-1
C
WT / WT
WT / cwg1-1
WT / bgs4Δ
cwg1-1 / cwg1-1
cwg1-1 / bgs4Δ
Phase contrast
Calcofluor
D
WT pAL
WT pAL-bgs4+
orb11-59 pAL
orb11-59 pAL-bgs4+
Phase contrast
Calcofluor

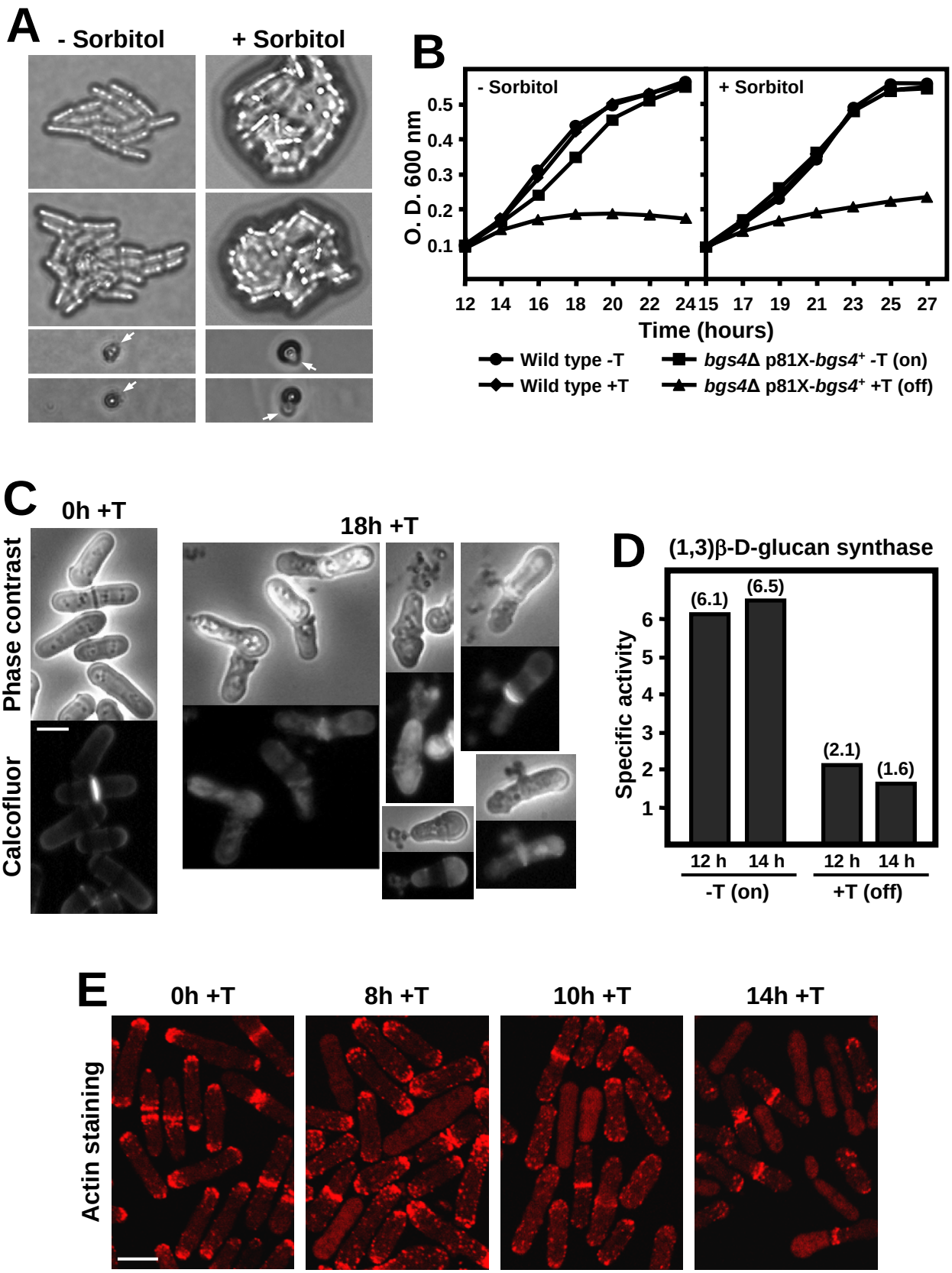
A
- Sorbitol
+ Sorbitol
B
- Sorbitol
+ Sorbitol
O. D. 600 nm
0.5
0.4
0.3
0.2
0.1
12 14 16 18 20 22 24 15 17 19 21 23 25 27
Time (hours)
Wild type -T
Wild type +T
bgs4Δ p81X-bgs4+ -T (on)
bgs4Δ p81X-bgs4+ +T (off)
C
0h +T
18h +T
Phase contrast
Calcofluor
D
(1,3)β-D-glucan synthase
Specific activity
6
5
4
3
2
1
(6.1)
(6.5)
(2.1)
(1.6)
12 h
14 h
12 h
14 h
-T (on)
+T (off)
E
0h +T
8h +T
10h +T
14h +T
Actin staining

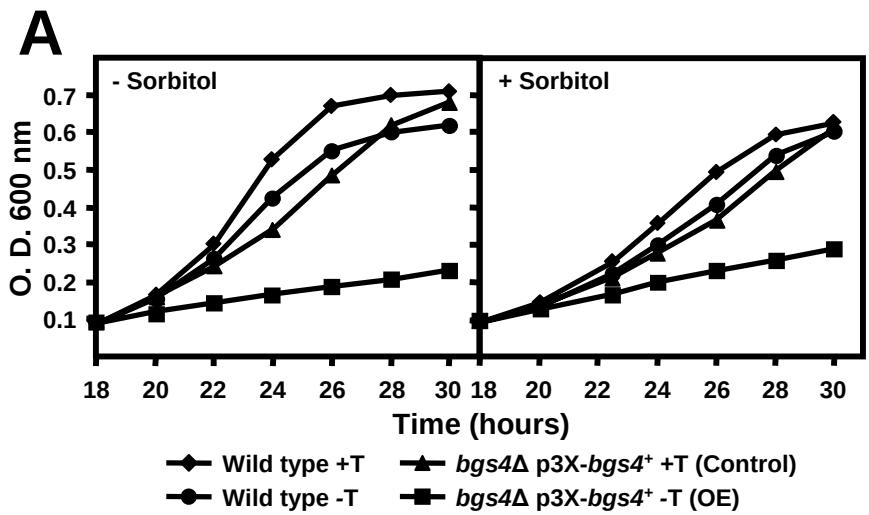
A
- Sorbitol
+ Sorbitol
O. D. 600 nm
0.7
0.6
0.5
0.4
0.3
0.2
0.1
18 20 22 24 26 28 30
Time (hours)
Wild type +T
Wild type -T
bgs4Δ p3X-bgs4+ +T (Control)
bgs4Δ p3X-bgs4+ -T (OE)

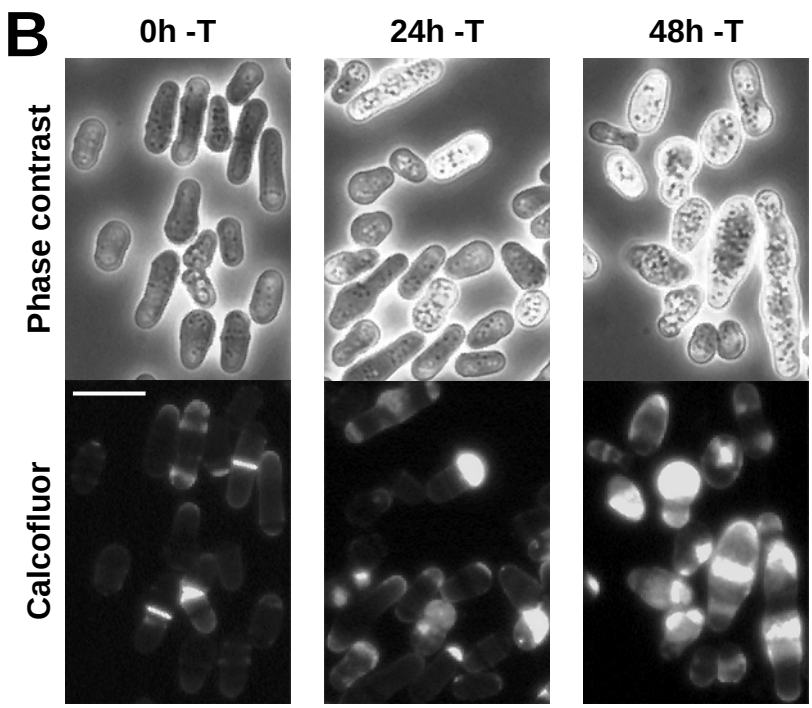
B
0h -T
24h -T
48h -T
Phase contrast
Calcofluor

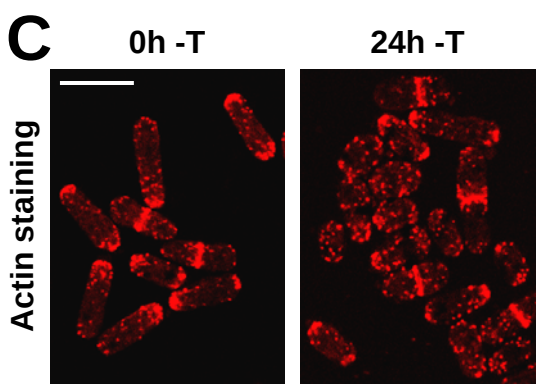
C
0h -T
24h -T
Actin staining

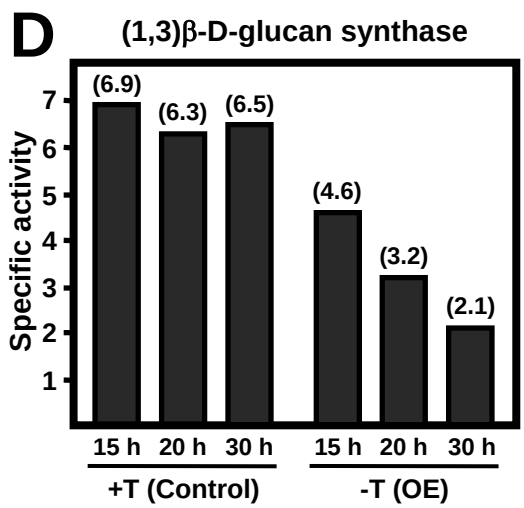
D
(1,3)β-D-glucan synthase
Specific activity
7
6
5
4
3
2
1
(6.9)
(6.3)
(6.5)
(4.6)
(3.2)
(2.1)
15 h 20 h 30 h
15 h 20 h 30 h
+T (Control)
-T (OE)

**Cortés *et al.* Fig. 4AB**

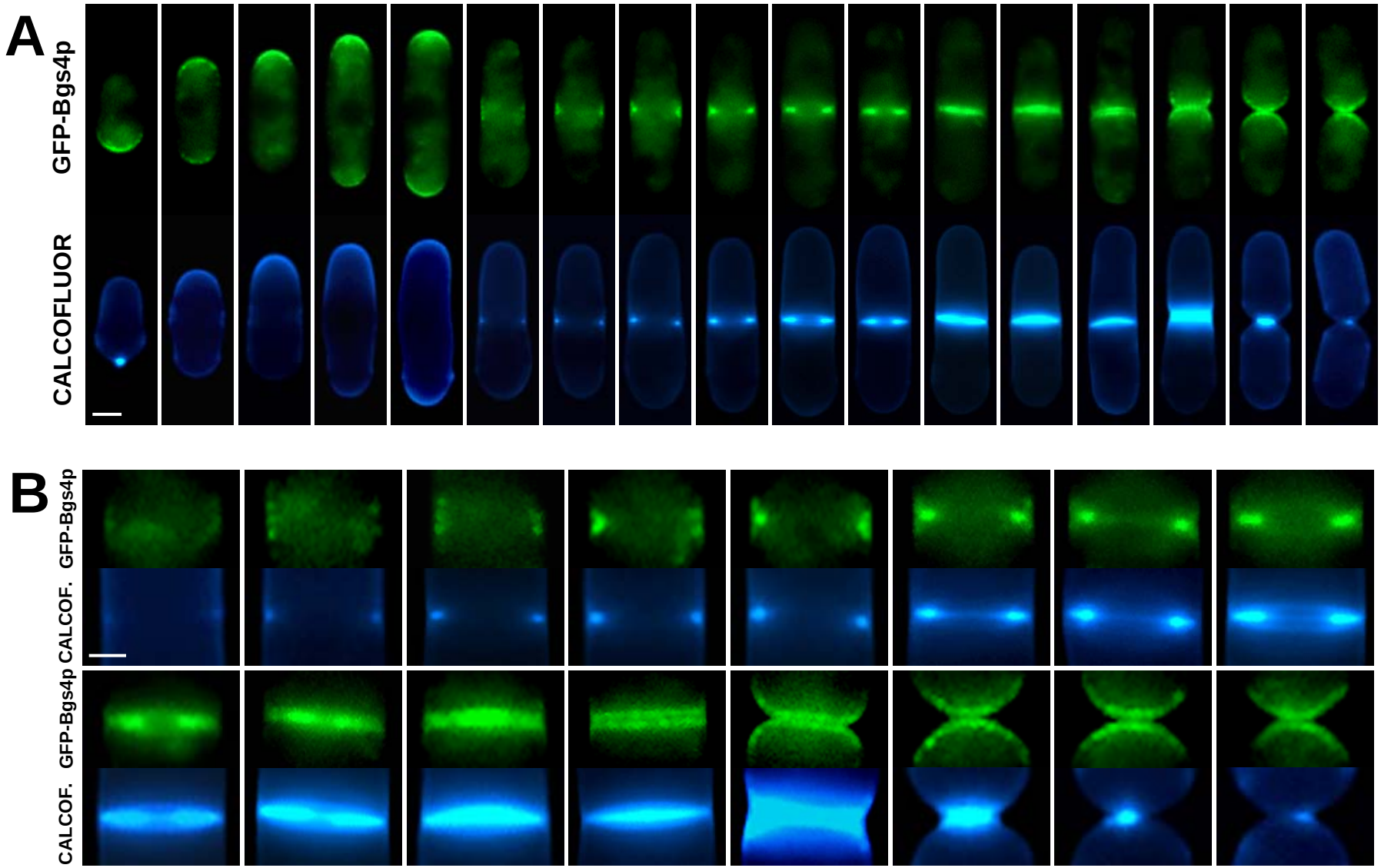

**Cortés *et al.* Fig. 4C**

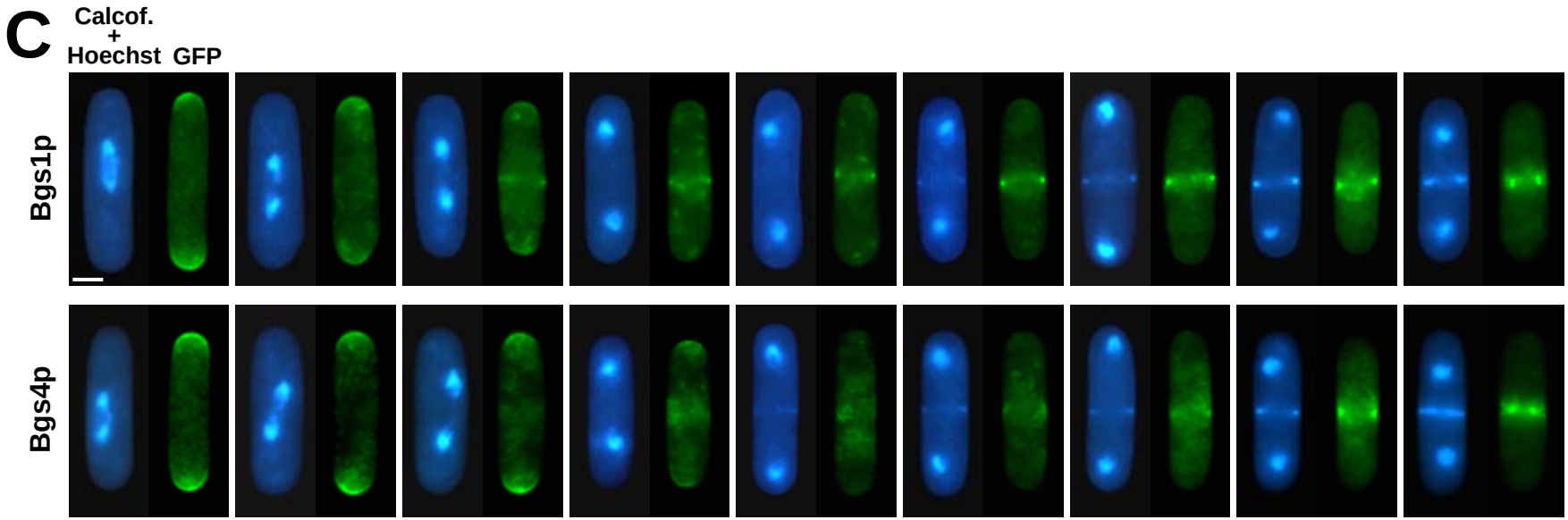

**Cortés *et al.* Fig. 5**

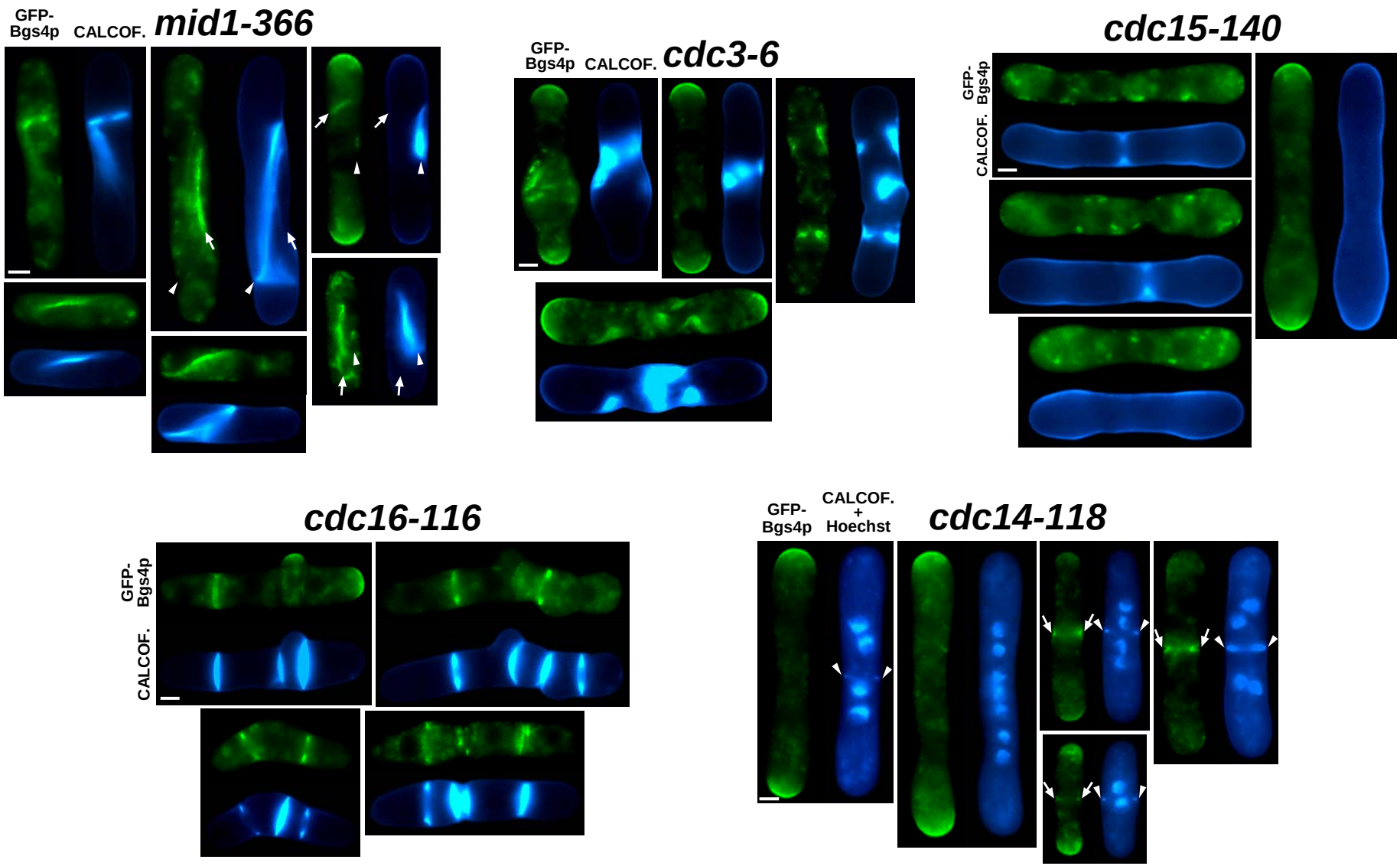

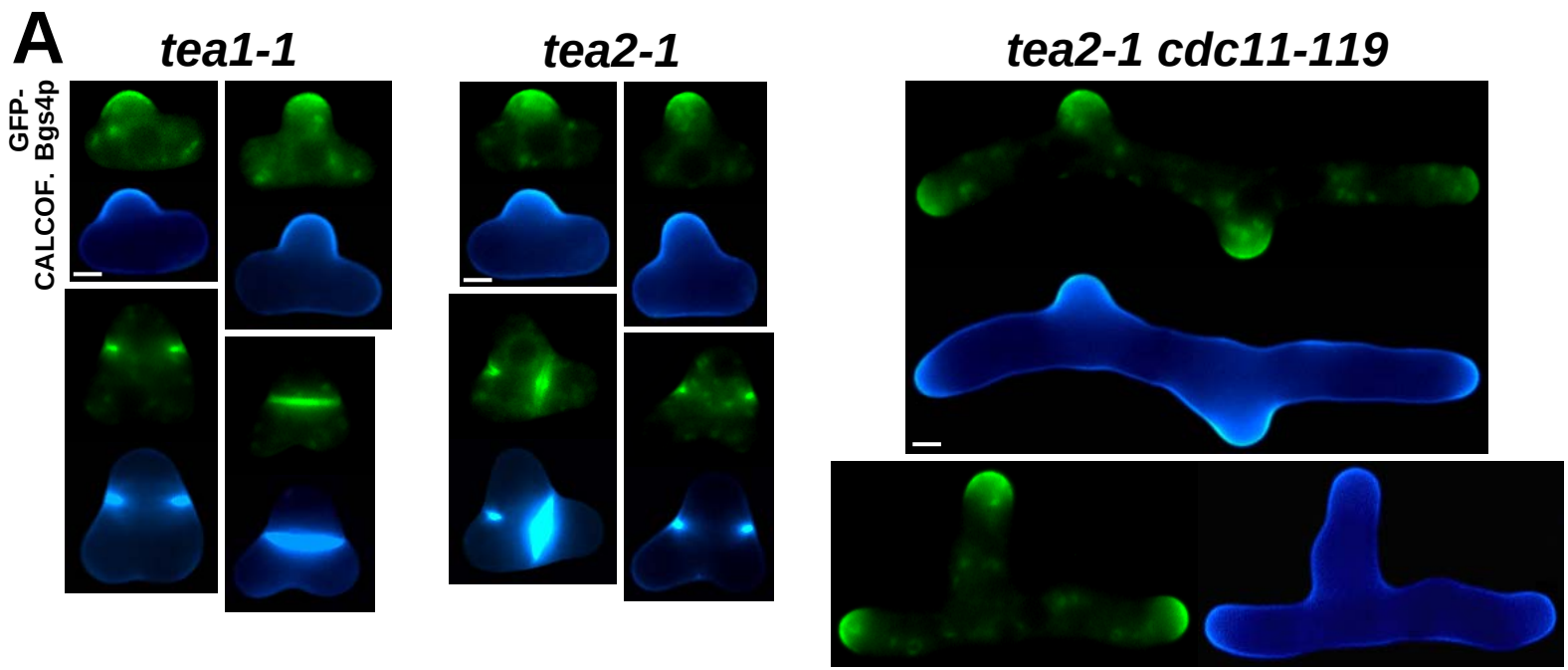
A
tea1-1
tea2-1
tea2-1 cdc11-119
GFP-Bgs4p
CALCOF.
B
cps8-188
GFP-Bgs4p
CALCOF.

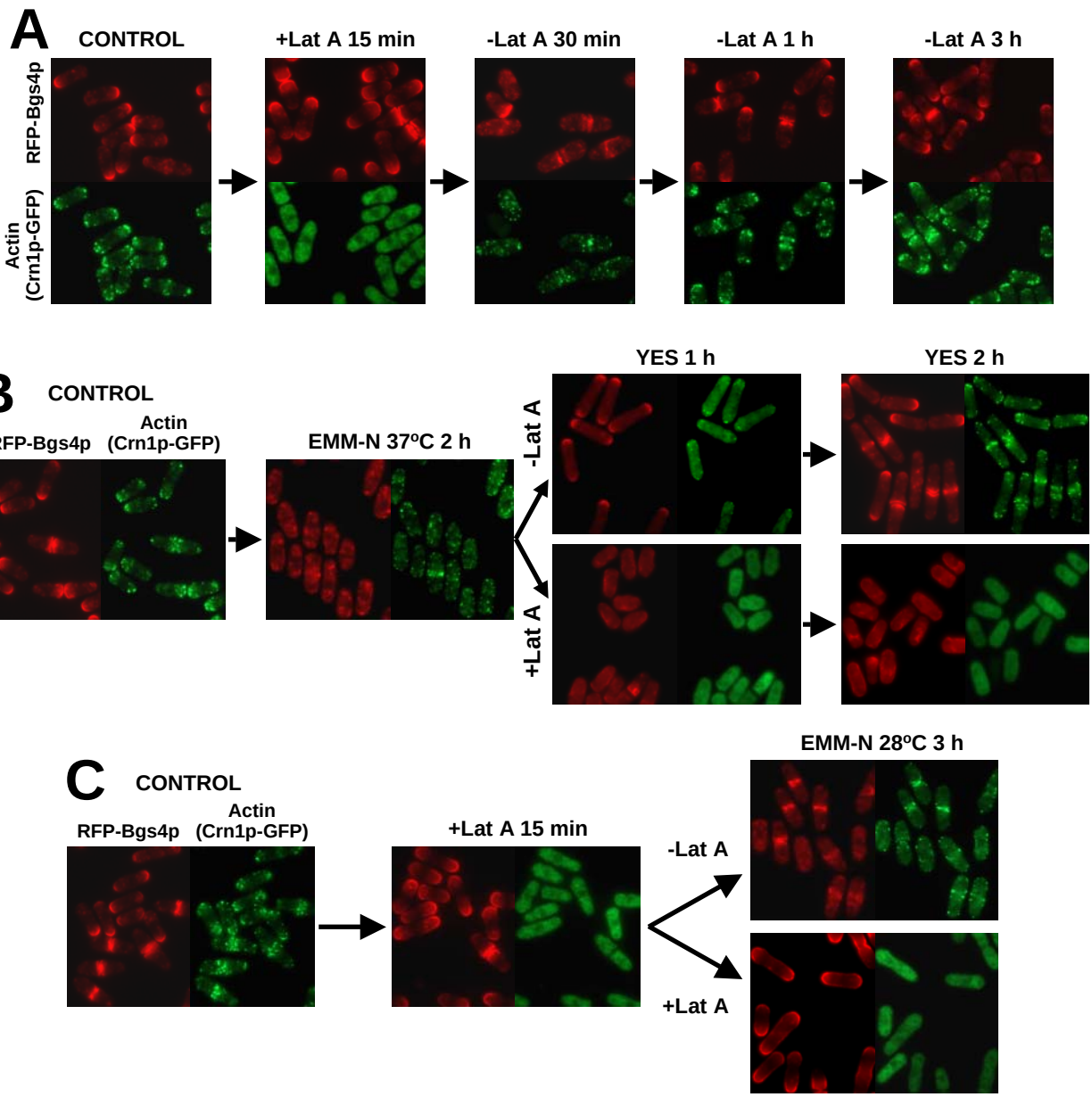
A
CONTROL
+Lat A 15 min
-Lat A 30 min
-Lat A 1 h
-Lat A 3 h
RFP-Bgs4p
Actin (Crn1p-GFP)
B
CONTROL
RFP-Bgs4p
Actin (Crn1p-GFP)
EMM-N 37ºC 2 h
YES 1 h
YES 2 h
-Lat A
+Lat A
C
CONTROL
RFP-Bgs4p
Actin (Crn1p-GFP)
+Lat A 15 min
EMM-N 28ºC 3 h
-Lat A
+Lat A

**Cortés *et al.* Fig. 8**

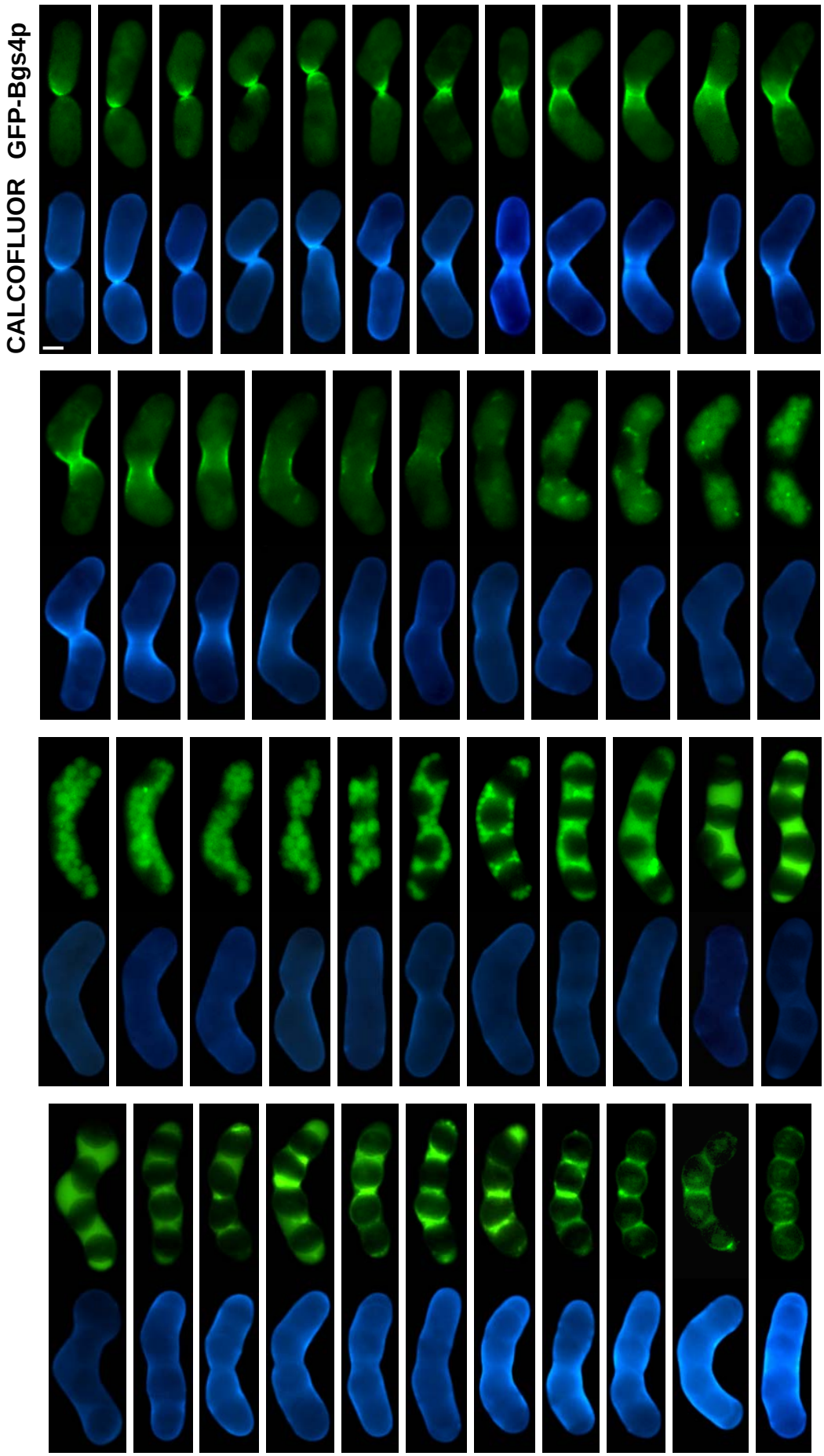

**Cortés *et al.* Fig. 9**

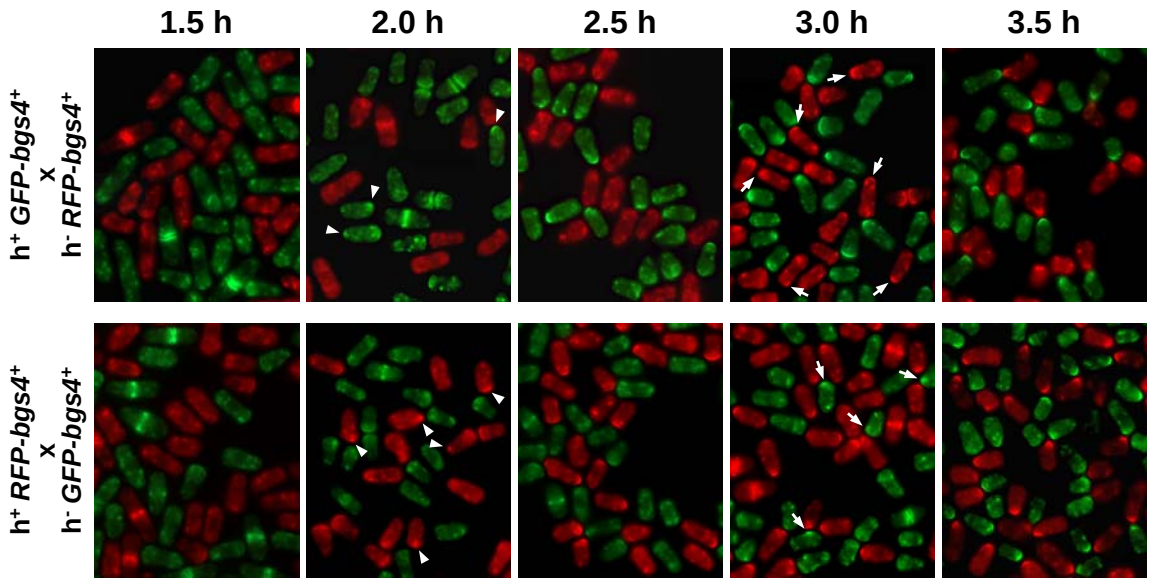

**Cortés *et al.* Fig. 10**